

POLYETHYLENEIMINE INTERLAYERED THIN FILM NANOCOMPOSITE
REVERSE OSMOSIS MEMBRANE FOR IMPROVED WATER DESALINATION

NG ZHI CHIEN

UNIVERSITI TEKNOLOGI MALAYSIA

POLYETHYLENEIMINE INTERLAYERED THIN FILM NANOCOMPOSITE
REVERSE OSMOSIS MEMBRANE FOR IMPROVED WATER DESALINATION

NG ZHI CHIEN

A thesis submitted in fulfilment of the
requirements for the award of the degree of
Doctor of Philosophy

School of Chemical and Energy Engineering
Faculty of Engineering
Universiti Teknologi Malaysia

AUGUST 2021

ACKNOWLEDGEMENT

First of all, I would like to thank and express my utmost gratitude to my supervisor, Assoc. Prof. Dr. Lau Woei Jye for providing endless support and useful opinion throughout the development of this research. His sharing of knowledge and his expertise in the field of membrane technology has given rise to the discovery of new ideas and solutions that enable smooth progress of my study. Meanwhile, his great values of being understanding and encouraging have become a moral support throughout my study period.

Besides, I would like to thank all my colleagues whom without their help, there will be no success in this research. Their sharing of experiences and knowledge enable me to overcome all obstacles during the studies. Moreover, I would like to thank my family for their everlasting support and understanding throughout my entire life. Without their support and blessing, the journey of this study would be difficult.

Last but not least, my greatest appreciation to the Zamalah Scholarship from Universiti Teknologi Malaysia (UTM) for funding my PhD studies.

ABSTRACT

Water desalination is the most effective strategy in dealing with global water crisis. However, the current thin film composite (TFC) reverse osmosis (RO) membranes which dominate the desalination process are still susceptible to permeability and selectivity trade-off, fouling and chlorine attack. These issues were resolved in this work by optimizing the synthesis conditions of interfacial polymerization (IP) technique for TFC membrane fabrication followed by adopting interlayer-assisted IP technique and graphene oxide (GO) incorporation for the fabrication of thin film nanocomposite (TFN) membrane. Polyethyleneimine (PEI) was used as interlayer for TFN membrane fabrication to avoid defects caused by GO incorporation in the polyamide (PA) layer. The effects of post IP rinsing on the TFC membrane were first investigated prior to the TFN membrane fabrication. It was found that the rinsing solution properties such as boiling point, surface tension and miscibility could affect the efficiency of unreacted monomers removal, altering the physicochemical properties of PA layer and yielding reproducible TFC membrane with higher water flux and least deteriorated salt rejection. Aqueous solution rinsing was found to be able to enhance membrane pure water flux (PWF) from 17.53 to 22.56 L/m²·h at 15 bar without significantly trading off its promising sodium chloride (NaCl) rejection (97.70%) when compared to the control membrane and organic solvent-rinsed membrane. For the TFN membrane, the presence of PEI interlayer was found to improve the distribution and orientation of GO in the PA layer which minimized the defects formed. Compared to the typical TFN membrane fabricated using conventional IP, the PEI-interlayered TFN membranes containing the same amount of GO (0.015 wt/v%) were found to exhibit a relatively thinner but rougher PA. As a result, almost all PEI-interlayered TFN membrane exhibited better desalination performances than the typical TFN membrane. It was also discovered that the substrate of membrane coated with a single layer of 0.05 wt/v% PEI followed by 60-min drying produced promising TFN membrane (i.e., iTFN-C0.05-T60-L1), achieving 96.66% NaCl rejection and 2.24 L/m²·h·bar PWF. The experimental results also revealed that the use of optimum GO loading (0.01 wt/v% GO) in the PA layer fabricated via interlayer-assisted IP could further improve TFN membrane performance, leading to the highest PWF (2.66 L/m²·h·bar) achieved without compromising NaCl rejection (~97.5%). This was caused by the improved membrane surface hydrophilicity and roughness paired with the nanochannels created by GO. The optimized TFN membrane also showed improved resistivity against alginate and least deteriorated desalination property after chlorination. Although the antibacterial property of GO was hindered by the PA layer, the membrane still exhibited better antibacterial property than that of commercial RO membrane. The outcomes of this study suggested that properly arranged GO in PA layer is necessary to minimize the formation of defects that could be detrimental for membrane separation. The position of GO in PA layer is particularly important to optimize its functionality. As a conclusion, the PEI-interlayered TFN membrane fabricated in this study portrayed a great potential in addressing the drawbacks of commercial TFC membrane for seawater or brackish water desalination.

ABSTRAK

Penyahgaraman air adalah strategi yang paling efektif dalam menangani krisis air global. Namun, membran osmosis berbalik (RO) komposit film nipis (TFC) yang mendominasi proses penyahgaraman kini masih terdedah kepada keseimbangan antara kebolehtelapan dan kememilihan, pengotoran dan serangan klorin. Masalah-masalah ini diselesaikan dalam kajian ini dengan mengoptimumkan keadaan teknik sintesis pemolimeran antaramuka (IP) untuk pembuatan membran TFC diikuti dengan menggunakan teknik antara lapisan berbantu IP dan penggabungan grafin oksida (GO) untuk fabrikasi membran komposit nano film nipis (TFN). Polietilenaimina (PEI) digunakan sebagai lapisan antara untuk fabrikasi membran TFN bagi mengelakkan ketidaksempurnaan yang disebabkan oleh penggabungan GO dengan lapisan poliamida (PA). Kesan pembilasan selepas IP pada membran TFC diselidiki terlebih dahulu sebelum fabrikasi membran TFN. Didapati bahawa sifat larutan bilas seperti suhu didih, tegangan permukaan dan kebolehcampuran boleh mempengaruhi kecekapan penyingkiran monomer yang tidak bertindak balas, mengubah sifat fizikokimia lapisan PA dan menghasilkan membran TFC yang boleh dihasilkan semula dengan fluks air yang lebih tinggi dan penolakan garam yang paling sedikit merosot. Pembilas larutan akueus didapati mampu meningkatkan PWF membran dari 17.53 hingga 22.56 L/m²·h pada 15 bar tanpa mengubah penolakan natrium klorida (NaCl) dengan ketara (97.70%) jika dibandingkan dengan membran kawalan dan membran yang dibilas oleh pelarut organik. Untuk membran TFN, kehadiran lapisan antara PEI didapati meningkatkan penyebaran dan orientasi GO dalam lapisan PA dan meminimumkan pembentukan ketidaksempurnaan. Dibandingkan dengan membran TFN biasa yang dibuat dengan menggunakan IP konvensional, membran TFN dengan lapisan antara PEI dengan kuantiti GO yang sama (0.015 wt/v%) mempunyai PA yang lebih nipis tetapi kasar. Hasilnya, hampir semua membran TFN dengan lapisan antara PEI menunjukkan prestasi penyahgaraman yang lebih baik daripada membran TFN biasa. Didapati bahawa substratum membran yang dimodifikasi dengan lapisan tunggal PEI sebanyak 0.05 wt/v% diikuti pengeringan 60-minut menghasilkan membran TFN (iaitu iTFN-C0.05-T60-L1) dengan prestasi penyahgaraman terbaik (96.66% penolakan NaCl dan 2.24 L/m²·h·bar). Hasil eksperimen juga menunjukkan bahawa penambahan GO yang optimum (0.01 wt/v% GO) dalam lapisan PA yang dibuat dengan teknik antara lapisan berbantu IP dapat menambahbaik prestasi membran TFN, memberi peningkatan dalam PWF (2.66 L/m²·h·bar), tanpa menjejaskan penolakan NaCl (~97.5%). Ini disebabkan oleh peningkatan kehidrofilikan dan kekasaran permukaan membran disamping saluran nano yang dibuat oleh GO. Membran TFN yang dioptimumkan ini juga menunjukkan ketahanan yang lebih baik terhadap alginat dan kemerosotan sifat penyahgaraman yang sedikit selepas pengklorinan. Walaupun sifat antibakteria GO dihalang oleh lapisan PA, membran ini masih menunjukkan sifat antibakteria yang lebih baik apabila dibandingkan dengan membran RO kelas komersial. Kajian ini menunjukkan bahawa GO yang disusun dengan betul dalam lapisan PA diperlukan untuk meminimumkan pembentukan ketidaksempurnaan yang boleh memudaratkan prestasi penyahgaraman membran. Kedudukan GO dalam lapisan PA penting untuk mengoptimumkan fungsinya. Sebagai kesimpulan, membran TFN dengan lapisan antara PEI yang dibuat dalam kajian ini mempunyai potensi besar dalam mengatasi kekurangan membran TFC komersial untuk penyahgaraman air laut atau air payau.

TABLE OF CONTENTS

	TITLE	PAGE
	DECLARATION	iii
	DEDICATION	iv
	ACKNOWLEDGEMENT	v
	ABSTRACT	vi
	ABSTRAK	vii
	TABLE OF CONTENTS	viii
	LIST OF TABLES	xiii
	LIST OF FIGURES	xiv
	LIST OF ABBREVIATIONS	xviii
	LIST OF SYMBOLS	xxiii
	LIST OF APPENDICES	xxvi
CHAPTER 1	INTRODUCTION	1
1.1	Background of Research	1
1.2	Problem Statements	6
1.3	Research Objectives	9
1.4	Research Scopes	9
1.5	Significance of Study	12
1.6	Assumptions and Limitations of Study	13
CHAPTER 2	LITERATURE REVIEW	15
2.1	Technologies for Seawater Desalination	15
2.1.1	Thermal-based Desalination Technology	17
2.1.2	Membrane-based Desalination Technology	17
2.2	Reverse Osmosis	19
2.2.1	Principles of Reverse Osmosis	19
2.2.1.1	Irreversible Thermodynamics Models	21

2.2.1.2	Porous Models	22
2.2.1.3	Non-Porous or Homogeneous Membrane Models	23
2.2.2	Important Inventions of Reverse Osmosis Membranes and Their Respective Pros and Cons	24
2.2.2.1	Cellulosic Membrane	25
2.2.2.2	Thin Film Composite Membrane	26
2.3	Interfacial Polymerization	28
2.3.1	Factors Affecting IP	30
2.3.1.1	Monomer Type, Molar Ratio and Concentration	30
2.3.1.2	Immersion and Reaction Time	37
2.3.1.3	Heat Treatment Conditions	38
2.3.1.4	Types of Organic Solvent	42
2.3.1.5	Post IP Rinsing	46
2.3.2	Conventional IP Technique	47
2.3.3	Comparison between Conventional IP and Interlayer-Assisted IP	48
2.3.3.1	A Potential Candidate for Interlayer-Assisted IP: Polyethyleneimine	50
2.4	Development of Thin Film Nanocomposite Membrane	55
2.4.1	Common Technique of TFN Membrane Fabrication and Their Limitations	56
2.4.2	Characteristics of Nanofillers for TFN Membrane Fabrication	57
2.4.2.1	Particle Size	57
2.4.2.2	Shape	57
2.4.2.3	Surface Chemistry and Hydrophilicity	59
2.4.2.4	Quantity	60
2.4.3	Impact of Nanofillers on Membrane Properties and Performances	61
2.4.3.1	Water Permeability and Solute Rejection	62

2.4.3.2	Organic and Inorganic Fouling Resistance	67
2.4.3.3	Chlorine Resistance	69
2.4.3.4	Antibacterial or Antimicrobial Property	70
2.5	Graphene Oxide as Nanofillers in the Polyamide	72
2.5.1	Synthesis Methods of GO	73
2.5.2	Formation Mechanisms of GO	75
2.5.3	Characteristics of GO	76
2.5.4	Development of GO Assisted TFN Membrane for RO Application and its Limitation	79
2.6	Overview and Research Gap	82
CHAPTER 3	RESEARCH METHODOLOGY	83
3.1	Introduction	83
3.2	Chemicals and Materials	83
3.3	Synthesis of GO	84
3.4	Fabrication of TFC and TFN membranes	86
3.4.1	Preparation of Commercial PSf Substrate	86
3.4.2	Fabrication of TFC Membrane via Conventional IP using Rubber Rolling Method by Varying the Type of Rinsing Solution and Rinsing Conditions	86
3.4.3	Fabrication of TFN Membrane via Conventional IP and Interlayer-Assisted IP using Oven-Drying Method by Varying PEI Coating Parameters	88
3.4.4	Fabrication of TFC and TFN Membranes via Interlayer-Assisted IP using Oven-Drying Method by Varying GO Loading	90
3.5	Characterization	91
3.5.1	Interlayer-spacing Analysis	91
3.5.2	Absorptivity Analysis	91
3.5.3	Morphology Analysis	91
3.5.4	Height Profile and Surface Roughness Analysis	92
3.5.5	Surface Chemistry Analysis	93

3.5.6	Surface Deposition and Elemental Analysis	93
3.5.7	Membrane Wettability Analysis	93
3.5.8	Surface Charge Analysis	94
3.5.9	Pore Size Estimation	94
3.5.10	MWCO	95
3.6	Performance Evaluation	95
3.6.1	Filtration Test	95
3.6.2	Fouling Test	96
3.6.3	Chlorine Resistivity Test	97
3.6.4	Antibacterial Test	98
CHAPTER 4	RESULTS AND DISCUSSION	101
4.1	Introduction	101
4.2	Fabrication of TFC Membranes: Effects of Rinsing Solution and Rinsing Conditions	102
4.2.1	Membrane Desalination Performance and Surface Hydrophilicity	102
4.2.2	Characterization of Membrane	106
4.2.2.1	Membrane Surface Chemistry	106
4.2.2.2	Membrane Surface Morphology	109
4.3	Fabrication of TFN Membranes: Effects of PEI Intermediate Layer and its Coating Conditions	111
4.3.1	Characterization of GO	111
4.3.2	Characterization of Membrane	113
4.3.2.1	Effects of PEI on the Physicochemical Properties of PSf Substrate	113
4.3.2.2	Effects of PEI Interlayer on the Physicochemical Properties of TFN Membrane	118
4.3.3	Membrane Desalination Performance	126
4.4	Fabrication of TFC and TFN Membranes via Interlayer-Assisted IP: Effects of GO Loading	129
4.4.1	Characterization of Membrane	129
4.4.1.1	Membrane Surface Chemistry	129

4.4.1.2	Membrane Surface Morphology	133
4.4.1.3	Membrane Surface Charge and Hydrophilicity	135
4.4.2	Membrane Desalination Performance	137
4.5	Performance Evaluation of iTFC and iTFN-10 Membranes	140
4.5.1	Chlorine Resistivity	140
4.5.2	Antifouling Property	142
4.5.3	Antibacterial Property	145
4.6	Summary	146
CHAPTER 5	CONCLUSIONS	149
5.1	Conclusions	149
5.2	Recommendations	151
	REFERENCES	155
	APPENDICES	185-195
	LIST OF PUBLICATIONS	197

LIST OF TABLES

TABLE NO.	TITLE	PAGE
Table 2.1	Typical constituents of seawater (Bahar and Hawlader, 2013)	16
Table 2.2	Global state of major seawater desalination processes (Koroneos <i>et al.</i> , 2012; Ng <i>et al.</i> , 2015; Williams <i>et al.</i> , 2015; Jones <i>et al.</i> , 2019)	18
Table 2.3	Properties of various organic solvents	43
Table 2.4	Important parameters for PEI coating deposition	54
Table 2.5	Structure and properties of GO based on the earliest and modern model (Dreyer <i>et al.</i> , 2010; Chua and Pumera, 2014)	78
Table 2.6	Properties and performances of GO-incorporated TFN membranes for RO application	80
Table 3.1	Conditions for TFC membranes preparation	87
Table 3.2	IP technique used and GO loading in preparing the composite membranes	90
Table 4.1	Properties of rinsing solutions	106
Table 4.2	Transmission intensity of -COOH of the selected membranes	108
Table 4.3	Contact angle and surface roughness of bare PSf and PEI-coated PSf substrates	116
Table 4.4	MWCO of bare and PEI-coated PSf substrates	118
Table 4.5	Contact angle and surface roughness of different TFN membranes	124

LIST OF FIGURES

FIGURE NO.	TITLE	PAGE
Figure 1.1	(A) Water withdrawal, GDP pro-capita and world population (Boretti and Rosa, 2019), (B) Estimated and projected trends of total blue water withdrawal, sectoral blue water consumption and ground water extraction over the period of 1960 to 2099 (Wada and Bierkens, 2014) and (C) graphical concept of water scarcity, resulting from a more than linear growing demand and a similarly more than a linear reduction of clean water availability (Boretti and Rosa, 2019)	2
Figure 1.2	Expansion of water-stressed region from year 2019 (Uhlenbrook <i>et al.</i> , 2020) to year 2040 (Luo, Young and Reig., 2015)	3
Figure 1.3	Number and capacity of operational desalination facilities by technology (Jones <i>et al.</i> , 2019)	4
Figure 2.1	Schematic diagram illustrating (A) RO process (Shenvi, Isloor and Ismail, 2015) and (B) direction of water flow in RO (Qasim <i>et al.</i> , 2019)	19
Figure 2.2	Aggregated pore and network pore detected using PALS (Ismail and Matsuura, 2018)	20
Figure 2.3	Schematic illustrations of asymmetric (A) Loeb-Sourirajan CA membrane and (B) TFC membrane	25
Figure 2.4	Schematic illustrations of (A) IP between MPD and TMC on the surface of a microporous support (Khorshidi <i>et al.</i> , 2016), (B) interface of two immiscible liquids (Raaijmakers and Benes, 2016) and (C) chemical structure of FAPA where n and m represent cross-linked and linear, respectively (Kang and Cao, 2012)	29
Figure 2.5	Scanning electron microscopy (SEM) images of (A) bottom surface and (B) top surface of the FAPA of a homemade RO membrane (Yan <i>et al.</i> , 2015)	30
Figure 2.6	Typical lab scale IP procedures for TFC flat sheet membrane fabrication (Seah <i>et al.</i> , 2020)	48
Figure 2.7	Chemical structure of (A) linear PEI and (B) branched PEI	51
Figure 2.8	Schematic illustration of TFN membrane	55

Figure 2.9	Schematic illustration of size exclusion effect and flow pattern of water across the TFN membrane incorporated with (A) MCM-41 and CNT (Yin <i>et al.</i> , 2012; Kim <i>et al.</i> , 2014; Baek <i>et al.</i> , 2017) and (B) GO and graphitic-CN (Inset: TEM image of respective nanofiller) (Gao <i>et al.</i> , 2017; Lai <i>et al.</i> , 2018, 2019)	63
Figure 2.10	FESEM (left) and AFM (right) images of TFC and TFN membranes incorporating with different nanofillers, (A) TNTs (0.05 wt/v%) (Chong <i>et al.</i> , 2019), (B) GO (0.02 wt%) (Yin, Zhu and Deng, 2016), (C) NH ₂ -MWCNT (0.05 wt%) (Vatanpour <i>et al.</i> , 2017) and (D) MMT (0.1 wt%) (Dong <i>et al.</i> , 2015)	66
Figure 2.11	(A) SEM observation of <i>P. aeruginosa</i> attached on TFC and CuBTri-modified TFN membranes in the dry contact assay (Wen <i>et al.</i> , 2019) and (B) Epifluorescence microscopy images of <i>E. coli</i> on TFC and GO-modified TFN membrane. The cells were stained in SYTO 9 (green) and Propidium Iodide (red) to represent live and dead cells, respectively (Inurria <i>et al.</i> , 2019)	72
Figure 2.12	Synthesis of GO via chemical oxidation process (Adetayo and Runsewe, 2019)	74
Figure 2.13	Schematic illustration of formation mechanism of GO from graphite (Hegab and Zou, 2015)	75
Figure 2.14	(A) Structure of GO based on Lerf-Klinowski model (He <i>et al.</i> , 1998) and (B) Types of interaction with GO (Fraga <i>et al.</i> , 2019)	77
Figure 3.1	Research flowchart	85
Figure 3.2	Schematic illustration of TFC membrane fabrication using 2 different rinsing approaches, (1) with rinsing and (2) with post air-drying and rinsing	88
Figure 4.1	Performance comparison of the neat TFC membrane (without rinsing) with the TFC membranes (with rinsing and with post air-drying and rinsing) using water and various organic solvents, (A) PWF and (B) NaCl rejection	105
Figure 4.2	Static contact angle of the neat TFC membrane (without rinsing) and the rinsed TFC membranes (with rinsing and with post air-drying and rinsing)	106
Figure 4.3	ATR-FTIR spectra comparison of the selected membranes, (A) without rinsing and with rinsing (TFC _{hex} and TFC _{water}) and (B) without rinsing and with post air-drying and rinsing (TFC _{drying+hex} and TFC _{drying+water})	108

Figure 4.4	FESEM images displaying the top surfaces (left) and cross-sections (middle) and AFM images demonstrating the surface roughness (right) of the selected membranes, (A) TFC, (B,C) TFC _{drying+hex} /TFC _{drying+water} and (D,E) TFC _{hex} /TFC _{water}	110
Figure 4.5	Structural characteristics of self-synthesized GO, (A) TEM images and (B) 2D AFM images and their corresponding height profiles	112
Figure 4.6	Characteristics of self-synthesized GO, (A) XRD spectrum, (B) FTIR spectrum and (C) UV-vis spectrum of 0.015 wt/v% GO aqueous solution and (D) Photos of 0.015 wt/v% graphite and GO dispersed in water	113
Figure 4.7	(A) ATR-FTIR analysis (Inset: narrow range (3200–3700 cm ⁻¹) of spectra and (B) zeta potential of PSf substrate with and without PEI coating	115
Figure 4.8	FESEM images of (A) bare PSf, (B) PEI-coated PSf substrate at the highest PEI concentration and (C) PEI-coated PSf substrate at the highest number of coating layers. The top surface and cross-sectional view are labelled as I and II, respectively	117
Figure 4.9	ATR-FTIR analysis of typical TFN membrane and PEI-interlayered TFN membranes at different wavenumbers: (A) 800–4000 cm ⁻¹ (broad range) and (B) 3200–3700 cm ⁻¹ (narrow range)	120
Figure 4.10	TEM images of (A) cTFN and (B) iTFN-C0.05-T60-L1 membranes scanned at two randomly selected regions, (I) region 1 and (II) region 2	121
Figure 4.11	FESEM images of (A) cTFN membrane and (B–H) PEI-interlayered TFN membranes synthesized under different conditions. The top surface and cross-sectional view are labelled as I and II, respectively	125
Figure 4.12	PWP and NaCl rejection of typical TFN and PEI-interlayered TFN membranes synthesized under different conditions, (A) PEI concentration, (B) PEI drying time and (C) number of PEI coating layer	128
Figure 4.13	ATR-FTIR spectra of typical TFC, PEI-interlayered TFC and TFN membranes at different wavenumber ranges: (A) 1400–4000 cm ⁻¹ (broad range) and (B) 3150–3600 cm ⁻¹ (narrow range)	130

Figure 4.14	(A) XPS analysis of cTFC, iTFC and iTFN-10 membranes and high-resolution spectra for (B, C and D) C1s and (E, F and G) N1s of the respective membrane. (I) is the XPS spectra whereas (II) is the elemental compositions and O/N ratio of cTFC, iTFC and iTFN-10 membranes	132
Figure 4.15	FESEM images of membrane top surface (left), cross section (middle) and AFM images (right) of (A) cTFC, (B) iTFC, (C) iTFN-5, (D) iTFN-10, (E) iTFN-15 and (F) iTFN-20	135
Figure 4.16	(A) Zeta potential and (B) contact angle of typical TFC, PEI-interlayered TFC and TFN membranes	137
Figure 4.17	(A-I) Desalination performances and (A-II) schematic illustration of the composite membranes. Performance comparison of (B) TFC and (C) TFN membranes from this work with other membranes reported in the literature. The commonly reported performance of commercial SWRO membrane and other lab-scale RO membranes is indicated using green dotted line and red dotted line, respectively Note: All information is extracted from articles with TFC (zero GO loading) and TFN membranes made using PSf as substrate and MPD and TMC as active monomers (Choi <i>et al.</i> , 2013; Perreault, Tousley and Elimelech, 2014; Chae <i>et al.</i> , 2015, 2017; He <i>et al.</i> , 2015; Kim <i>et al.</i> , 2016; Yin, Zhu and Deng, 2016; Ali <i>et al.</i> , 2016; Shao <i>et al.</i> , 2017; Xu <i>et al.</i> , 2019; Inurria <i>et al.</i> , 2019; Yang, Guo and Tang, 2019; Zhang <i>et al.</i> , 2020a; Rodríguez <i>et al.</i> , 2020). Both TFC and TFN membranes are extracted from the same article, whereby TFC is the membrane without GO while TFN is the best performing membrane with GO appears either within/atop PA layer or between PA and substrate.	139
Figure 4.18	(A) Water permeability and (B) salt rejection of iTFC and iTFN-10 membranes and normalized ATR-FTIR spectra of (C) iTFC membrane and (D) iTFN-10 membrane before and after chlorine exposure. The membranes were exposed to 500 and 1000 mg/L of NaOCl solution (pH ~10) for 24 h. Note: The 0 mg/L is referred to RO water without NaOCl.	142
Figure 4.19	(A) Fouling behaviour as a function of time and (B) FRR measured at the end of every fouling cycle of iTFC and iTFN-10 membranes. SEM images EDX analysis of (C) iTFC and (D) iTFN-10 membranes are labelled as I and II, respectively	144
Figure 4.20	(A) Bacterial inhibition rate and (B) concentrations of <i>E. coli</i> (top) and <i>S. aureus</i> (bottom) colonies deposited on the agar plates after a 24-h and 48-h incubation, respectively, for the iTFC and iTFN-10 membranes	146

LIST OF ABBREVIATIONS

2D	-	two dimensional
3D	-	three dimensional
AAPTS	-	1-(2-amino-ethyl)-3-aminopropyl] trimethoxysilane
AFM	-	atomic force microscopy
Ag	-	silver
ALD	-	atomic layer deposition
ATR	-	attenuated total reflectance
BaCl ₂ .2H ₂ O	-	barium chloride 2-hydrate
BaSO ₄	-	barium sulfate
BN	-	boron nitride
BSA	-	bovine serum albumin
<i>B. subtilis</i>	-	<i>Bacillus subtilis</i>
BTCE	-	biphenyl acid chloride
CA	-	cellulose acetate
CD	-	carbon dot
CDA	-	cellulose diacetate
CeO ₂	-	cerium oxide
CFIC	-	5-chloroformyloxy-isophthaloyl chloride
ClO ₂	-	chlorine dioxide
CN	-	carbon nitride
CNC	-	cellulose nanocrystal
CNT	-	carbon nanotube
COF	-	carbon organic framework
CP	-	concentration polarization
CTA	-	cellulose triacetate
Cu	-	copper
CuO	-	copper oxide
DABA	-	triamine 3,5-diamino-N-(4-aminophenyl) benzamide
DI	-	deionized
DNA	-	deoxyribonucleic acid

<i>E. coli</i>	-	<i>Escherichia Coli</i>
ED	-	Electrodialysis
EDA	-	ethylenediamine
EDX	-	elemental dispersive X-ray
EG	-	ethylene glycol
FAPA	-	fully aromatic polyamide
FESEM	-	field emission scanning electron microscopy
FO	-	forward osmosis
FTIR	-	Fourier transform infrared spectroscopy
GDP	-	gross domestic product
GO	-	graphene oxide
GQD	-	graphene quantum dot
HCl	-	hydrochloric acid
HDH	-	Humidification-dehumidification
HEMA	-	2-hydroxyethyl methacrylate
HFBA	-	2,2,3,4,4,4-hexafluorobutylacrylate
HNO ₃	-	nitric acid
HNT	-	halloysite nanotube
H ₂ O ₂	-	hydrogen peroxide
hPAN	-	hydrolyzed polyacrylonitrile
H ₂ SO ₄	-	sulfuric acid
HSO ₄ ⁻	-	hydrogen sulfate
ICIC	-	5-isocyanato-isophthaloyl chloride
IP	-	interfacial polymerization
IPC	-	isophthaloyl chloride
KBr	-	potassium bromide
KCl	-	potassium chloride
KClO ₃	-	potassium chlorate
KH ₂ PO ₄	-	potassium dihydrogen phosphate
KMnO ₄	-	potassium permanganate
LBL	-	layer-by-layer
LDH	-	layered double hydroxide
MED	-	multi-effect distillation

MF	-	microfiltration
MgCl ₂	-	magnesium chloride
MMT	-	montmorillonite
Mn ₂ O ₇	-	dimanganese heptoxide
mmBTEC	-	3,3',5,5'-biphenyl tetraacyl chloride
mNT	-	modified nanoporous titanate
MOF	-	metal organic framework
MoS ₂	-	molybdenum disulfide
MPD	-	m-phenylenediamine
MPIA	-	polymetaphenylene isophthalamide
MPTA	-	polymetaphenylene trimesamide
MSF	-	multi-stage flash distillation
MW	-	molecular weight
MWCNT	-	multiwalled carbon nanotube
MWCO	-	molecular weight cut-off
NaAlg	-	sodium alginate
NaCl	-	sodium chloride
Na ₂ CO ₃	-	sodium carbonate
Na ₂ HPO ₄	-	disodium hydrogen phosphate
NaNO ₃	-	sodium nitrate
NaOCl	-	sodium hypochlorite
NaOH	-	sodium hydroxide
NF	-	nanofiltration
NO ₂	-	nitrogen dioxide
NO ₃ ⁻	-	nitrate
N ₂ O ₄	-	dinitrogen tetroxide
OPD	-	o-phenylenediamine
OSN	-	organic solvent nanofiltration
PA	-	polyamide
PAA	-	polyacrylic acid
<i>P.aeruginosa</i>	-	<i>Pseudomonas aeruginosa</i>
Pal	-	palygorskite
PALS	-	Positron Annihilation Spectroscopy

PBS	-	phosphate-buffered saline
PDA	-	polydopamine
PE	-	polyelectrolyte
PEG	-	polyethylene glycol
PEI	-	polyethyleneimine
PES	-	polyethersulfone
PET	-	polyester
PFDTES	-	1H,1H,2H,2H-perfluorodecyltriethoxysilane
PFM	-	Pore Flow model
PI	-	polyimide
PIP	-	piperazine
PPD	-	p-phenylenediamine
<i>P. putida</i>	-	<i>Pseudomonas putida</i>
PSf	-	polysulfone
PV	-	pervaporation
PVA	-	polyvinyl alcohol
PVDF	-	polyvinylidene fluoride
PWF	-	pure water flux
PWP	-	pure water permeability
RNA	-	ribonucleic acid
RO	-	reverse osmosis
ROS	-	reactive oxygen species
SANS	-	Small-Angle Neutron Scattering
<i>S. aureus</i>	-	<i>Staphylococcus aureus</i>
SD	-	solar distillation
SDM	-	Solution-Diffusion model
SEM	-	scanning electron microscopy
SKM	-	Spiegler-Kedem model
TDS	-	total dissolved solid
TEM	-	transmission electron spectroscopy
TiO ₂	-	Titanium dioxide
TFC	-	thin film composite
TFN	-	thin film nanocomposite

TMC	-	trimesoyl chloride
TNS	-	titania nanosheet
TNT	-	titania nanotube
TOC	-	total organic carbon
UF	-	ultrafiltration
UV-Vis	-	ultraviolet-visible
VC	-	vapor compression
WHO	-	World Health Organization
XPS	-	X-ray photoelectron spectroscopy
XRD	-	X-ray diffraction
ZnO	-	zinc oxide

LIST OF SYMBOLS

A_s	-	solvent transport parameter
A	-	permeability
A_m	-	effective area of membrane
A_{w1}	-	initial membrane water permeability
A_{w2}	-	membrane water permeability after washing
B	-	solute transport parameter
C	-	mean concentration over the thickness of the membrane
C_I	-	ion concentration
C_f	-	solute/salt concentration in the feed solution
C_p	-	solute/salt concentration in the permeate solution
C_w	-	concentration of dissolved water in membrane
C_m	-	concentration of solute in the fluid at the feed/membrane interface
D_v	-	solvent diffusivity
D_s	-	solute diffusivity
d-spacing	-	interlayer spacing
FRR	-	flux recovery rate
I	-	bacterial inhibition rate
J	-	flux
J_v	-	solvent flux
J_s	-	solute flux
K_s	-	solute partition coefficient between the solution and membrane phases
K_S	-	absorption of salt
L	-	solvent permeability coefficient
N_m	-	bacterial concentration of the membrane sample on the agar plate
N_o	-	bacterial concentration of the blank sample on the agar plate
P'	-	local solute permeability
P	-	solute permeability
p_f	-	feed pressure

p_p	-	permeate pressure
R	-	rejection
r	-	ratio of actual area to the projected area of the surface
R_a	-	average roughness
R_i	-	ideal gas constant
R_r	-	real retention
R_D	-	dilution ratio
R_s	-	solute rejection
R_v	-	recovery
RMS	-	root mean square roughness
S_v	-	solvent solubility
T	-	temperature
TOC_f	-	TOC of solute in feed
TOC_p	-	TOC of solute in permeate
V_v	-	solvent partial molar volume
Z	-	number of visible bacteria colonies on the agar plate
σ	-	reflection coefficient
δ	-	pore length
π	-	osmotic pressure
Δp	-	transmembrane pressure difference
Δt	-	collection time of permeate
ΔV	-	volume of permeate
Δx	-	membrane thickness
$\Delta \pi$	-	osmotic pressure difference between the feed and permeate
γ	-	liquid/gas surface tension
γ_{sl}	-	solid/liquid interfacial energy
γ_{so}	-	solid/gas surface energy
γ_s^P	-	polar force of surface tension
Y	-	surface tension
μ	-	viscosity

θ	-	diffraction angle of nanofiller peak
θ^*	-	apparent contact angle
θ_Y	-	equilibrium contact angle
λ	-	irradiation wavelength in X-ray diffraction spectrometer
ρ	-	density

LIST OF APPENDICES

APPENDIX	TITLE	PAGE
Appendix A	Pore Radii Estimation of TFC Membranes	185
Appendix B	Zeta Potential of PEI	189
Appendix C	MWCO of PSf and PEI-coated PSf Substrate	190
Appendix D	Photographic Images of MPD-GO soaked PSf and PEI-coated PSf Substrates	191
Appendix E	Surface Charge of GO	192
Appendix F	Interactions between PEI with MPD	193
Appendix G	FESEM and AFM Images of iTFN-20 Membrane	194
Appendix H	Antibacterial Property of Commercial SWRO	195

CHAPTER 1

INTRODUCTION

1.1 Background of Research

Water crisis has become a threatening issue in many parts of the world despite the Earth is covered by 75% of water (Ali *et al.*, 2018). 97.5% of the 75% is made up of seawater and saline aquifers (Zaidi *et al.*, 2015) while fresh water only comprises of 2.5%. Out of the 2.5% of fresh water, only 0.3% is usable by human (Youssef, Al-Dadah and Mahmoud, 2014). The situation worsens when the available conventional freshwater resources are polluted by human activities and overexploited. In the 20th century, human population increases by four times but the demand for water has increased by nine times (Shenvi, Isloor and Ismail, 2015).

Figures 1.1A and 1.1B show the water withdrawal, gross domestic product (GDP) pro-capita and world population and the breakdown of human water consumption from various sectors while Figure 1.1C demonstrates the graphical concept of water crisis when demand is continuously increased while clean water availability is decreasing. The linear relationship of water withdrawal and world population, as observed in Figure 1.1A, further confirms that human population is the primary factor for the increase in global water demand. The global water withdrawal, which is in line with the sectoral water consumption, is predicted to rise continuously, with no sign of slowing down, until ~2099 (see Figure 1.1B). The drastic rise in irrigation and livestock water consumption is attributable to the increasing food demand, while the surge in domestic and industrial water use is ascribed to the increase in electricity and energy usage. Climate change is another factor that contributes to the remarkably high irrigation water consumption (Wada and Bierkens, 2014). It is intuitive that the growing demand and shrinking water availability will ultimately cross each other (see Figure 1.1C) when water withdrawal rate overcomes the nature's self-replenishing rate. At that moment, water crisis happens.

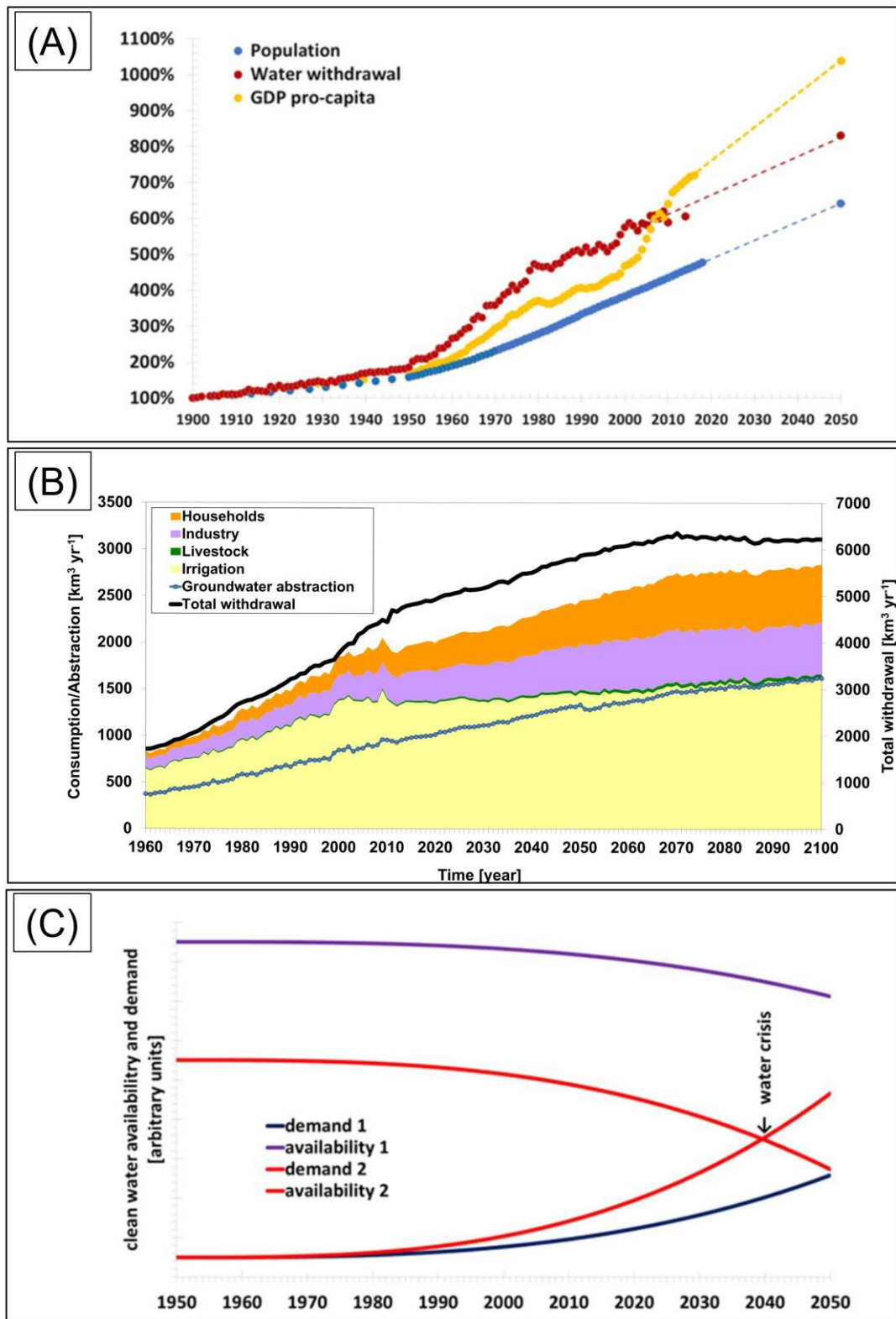


Figure 1.1 (A) Water withdrawal, GDP pro-capita and world population (Boretti and Rosa, 2019), (B) Estimated and projected trends of total blue water withdrawal, sectoral blue water consumption and ground water extraction over the period of 1960 to 2099 (Wada and Bierkens, 2014) and (C) graphical concept of water scarcity, resulting from a more than linear growing demand and a similarly more than a linear reduction of clean water availability (Boretti and Rosa, 2019)

It was previously mentioned by Service (2006) in his article “Desalination Freshens Up” that over 1 billion of people did not have access to clean drinking water and approximately 2.3 billion of people, which were about 41% of world population, were living in water stress region. It is also revealed in the United Nations World Water Development Report Edition 2018 that approximately 6 billion of people will suffer from clean water scarcity in 2050. Figure 1.2 predicts expansion of water stress region from 2019 to 2050. Based on the Global Risk report, water crisis has been listed and remained as the top 5 risk by severity of impact since 2014 (Brende, 2020).

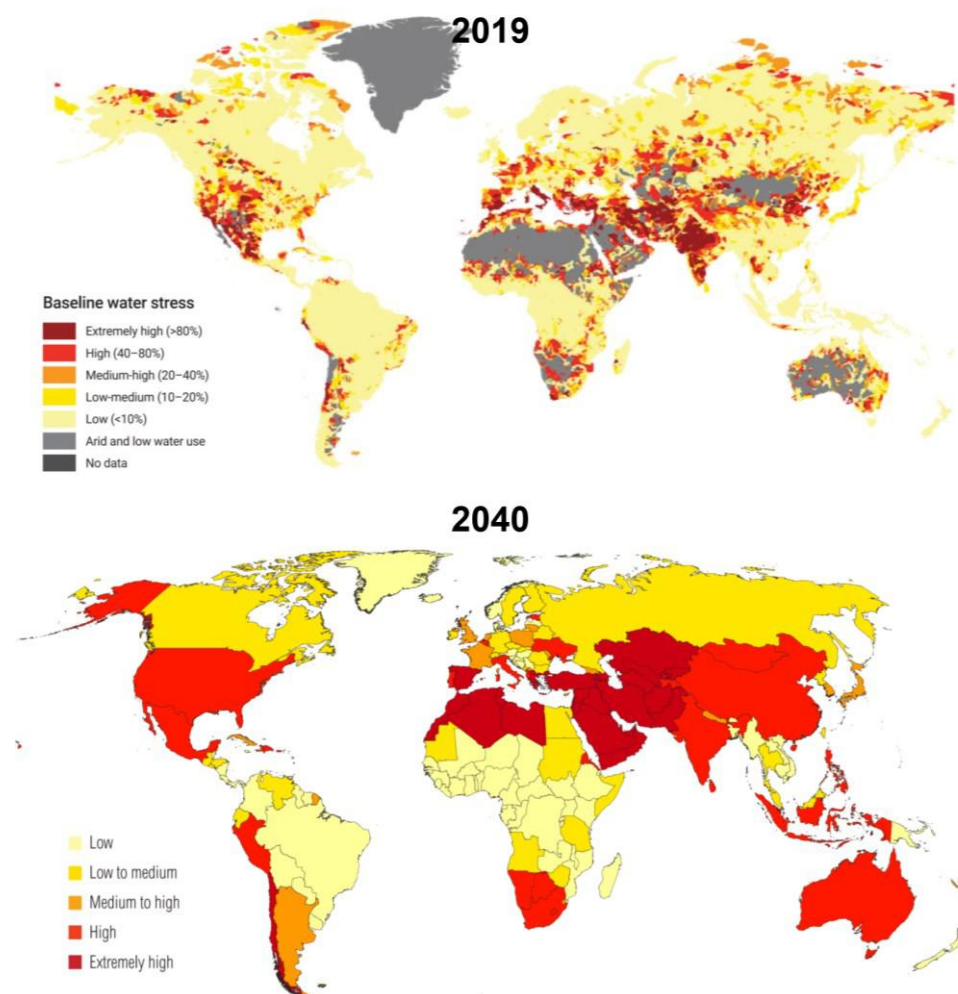


Figure 1.2 Expansion of water-stressed region from year 2019 (Uhlenbrook *et al.*, 2020) to year 2040 (Luo, Young and Reig., 2015)

The water crisis issue has urged mankind to search for a solution in resolving the Earth’s meagered fresh water supplies, leading to the development of water reuse and water desalination (Jiang, Li and Ladewig, 2017). Water reuse has been widely

applied to produce freshwater for irrigation, industrial activities, recharging of ground water and as a method for indirect drinking water production. Meanwhile, water desalination remains as the most preferred choice for drinking water production due to its ability to produce freshwater that fulfils the drinking water standard of the World Health Organization (WHO) (Greenlee *et al.*, 2009).

The two commonly applied desalination technologies are membrane-based technology and thermal-based technology. However, due to high energy consumption of thermal-based technology, membrane-based technology is more preferred. Membrane-based technology which is pressure-activated utilizes high pressure to force water across semipermeable membrane and leave salts behind (Youssef, Al-Dadah and Mahmoud, 2014). Reverse osmosis (RO) is currently the most promising membrane-based desalination technology. Besides being energy saving, RO also exhibits excellent separation performance with high water permeability fulfilling the demand of human population (Jiang, Li and Ladewig, 2017). Figure 1.3 shows the number and capacity of operational desalination plants by technology. According to Jones *et al.* (2019), RO is the most dominating process that accounts for 84% of the total number of operational desalination plants and produces 69% of global desalinated water.

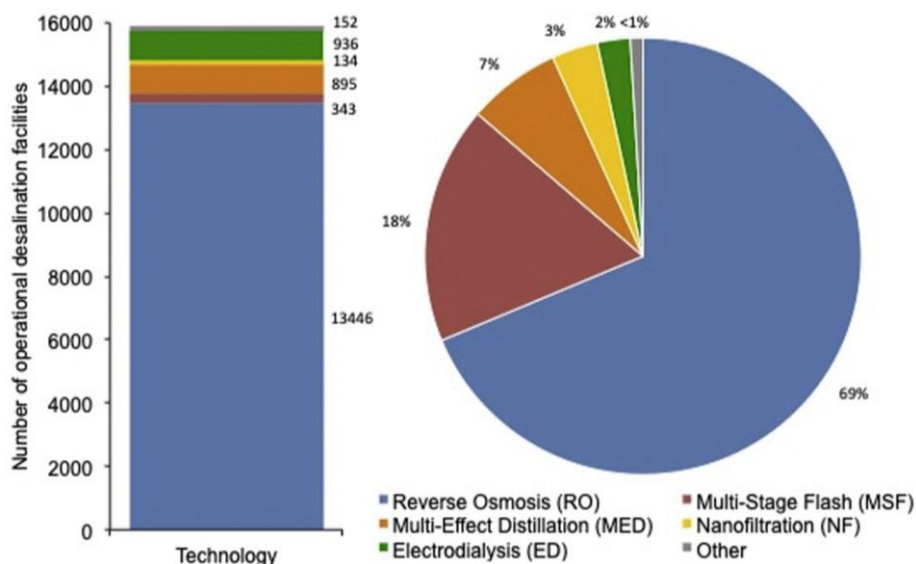


Figure 1.3 Number and capacity of operational desalination facilities by technology (Jones *et al.*, 2019)

To date, desalination technology is dominated by thin film composite (TFC) polyamide (PA) RO membranes (Lee, Arnot and Mattia, 2011), which was introduced by Cadotte and his co-workers in the 1970s (Cadotte *et al.*, 1980). This type of membrane consists of three layers, ultrathin PA layer, porous substrate and non-woven polyester (PET) fabric that is prepared via interfacial polymerization (IP) method. It exhibits excellent salt rejection of >99% and relatively higher water permeability, $\sim 0.74 \text{ L/m}^2 \cdot \text{h} \cdot \text{bar}$ as compared to asymmetric RO membranes. TFC membrane also exhibits better tolerance to temperature, chemical, wider range of pH and compaction. Nevertheless, the TFC membrane is subject to ubiquitous trade-off relationship between permeability and selectivity which hinders the simultaneous improvement of membrane water permeability and solute rejection. Apart from that, the TFC membrane is also susceptible to fouling and chlorine attack (Li, Yan and Wang, 2016). Following this, numerous studies were carried out by membrane scientists to address its drawbacks by modifying the structural properties and surface chemistry of TFC membrane, aiming to increase its resistibility against potential foulants and free active chlorine as well as improving its water permeability. Interlayer regulated IP process is one of the emerging strategies to improve the performances of TFC membrane (Dai, Li and Wang, 2020; Ng *et al.*, 2021). Compared to the conventional IP, interlayer-assisted IP usually produces PA which is thinner, smoother and more compact. These features grant the resultant TFC membrane its higher water permeability and salt rejection (Dai, Li and Wang, 2020).

Another effective strategy is to integrate inorganic nanofillers into the ultrathin barrier layer, resulting in the development of new type of composite membrane named as thin film nanocomposite (TFN) membrane. The nanofillers can be added into the selective PA layer via IP method. Addition of nanofillers is not only able to improve membrane water permeability, but also prevent the membrane selectivity from being compromised, as initially reported by Jeong *et al.* (2007). Apart from that, the incorporation of nanofillers could improve membrane antifouling, chlorine resistivity, antibacterial, mechanical property and thermal resistivity. Some of the inorganic nanofillers investigated include carbon-based (e.g., carbon nanotube (CNT), graphene oxide (GO)), metal and metal oxides-based (e.g., silver (Ag), copper (Cu), titanium dioxide (TiO₂), zinc oxide (ZnO) and metal organic framework (MOF)), silica, zeolite and halloysite nanotube (HNT) (Saleem and Zaidi, 2020).

Lately, GO has become one of the promising nanofillers for the development of TFN RO membrane (Liu and Xu, 2016). GO is attractive due to two main reasons, i.e., unique structure and superior hydrophilicity (Liu and Xu, 2016; Akther *et al.*, 2020). Its two dimensional (2D), single atom-thick sheet-like structure is capable of creating additional channels for water to pass through when they are stacked (Choi *et al.*, 2013). Meanwhile, the existence of abundant oxygen functional entities such as hydroxyl, epoxy and carboxyl groups locating at the surfaces and edges of GO could make it highly hydrophilic (Dreyer *et al.*, 2010; Shamaila, Sajjad and Iqbal, 2016; Inurria *et al.*, 2019). These properties provide the resultant TFN membrane with enhanced surface hydrophilicity, leading to improved permeability and antifouling property, when the GO is incorporated into the PA layer. Besides, the ability of GO to form intermolecular hydrogen bonding with PA layer could prevent the amide bond from being attacked by free chlorine (Ali *et al.*, 2016). GO also possesses antimicrobial property which is useful in mitigating biofouling of the resultant TFN membrane (Inurria *et al.*, 2019). Direct contact of bacteria with GO nanosheets results in the disruption of the cell membrane integrity and the oxidation of cellular components, which can induce loss of cell viability (Li *et al.*, 2011; Sanchez *et al.*, 2012; Mangadlao *et al.*, 2015). Albeit all the advantages of GO incorporated TFN membranes, there remains some limitations in the membrane properties that needed to be addressed such as incomplete accommodation, uneven distribution and random arrangement within the PA layer (Lai *et al.*, 2019; Lim *et al.*, 2020; Rodríguez *et al.*, 2020). Therefore, this study aims to investigate the combine effects of intermediate layer and GO incorporation on the physicochemical properties and performances of the resultant TFN membranes for desalination process. The effects of intermediate layer on the deposition of GO in the PA layer are explored.

1.2 Problem Statements

IP technique is widely employed for TFC and TFN membranes fabrication. Generally, it involves the reaction of two monomers (i.e., amine in aqueous medium and acyl chloride in organic medium) at the interface of two immiscible solutions to produce a thin and dense PA layer followed by heat treatment to improve the cross-

linking degree and remove excess solvents (Ghosh *et al.*, 2008). Nevertheless, the current TFC membrane still suffers from permeability/selectivity trade-off, chlorine attack and fouling. To deal with these problems, studies were conducted to alter the physicochemical properties of TFC membrane, among which varying PA synthesis conditions (i.e., IP parameters) and nanofillers incorporation (Xu, Wang and Li, 2013; Otitoju, Saari and Ahmad, 2018) are some of the effective strategies. Lately, the potential of post IP rinsing in improving water flux at the expense of solute rejection of TFC membrane was reported by Chong *et al.* (2018). Post IP rinsing is often required to remove unreacted monomers from the TFC membrane surface prior to heat treatment process. However, its effects on membrane physicochemical properties remain largely unclear. Thus, the first part of this research intends to study in depth the effects of post IP rinsing on the physicochemical properties and performances of TFC membranes by using various organic solvents (i.e., hexane, cyclohexane and Isoparaffin-G) to compare with water at different rinsing conditions (i.e., with rinsing (meaning the membrane is immediately rinsed after IP) and with post air-drying and rinsing (meaning the membrane is subjected to 1 min air-drying after IP before subjecting to rinsing)). It is anticipated that highly reproducible TFC membranes with insignificant permeability/selectivity trade-off could be fabricated and serve as a stable baseline for the development of PEI-interlayered TFN membranes.

In this study, GO nanosheets are proposed as the nanofillers for the fabrication of TFN membrane owing to its unique structure and superior hydrophilicity (containing an abundance of oxygen rich functional groups). Nevertheless, there remain several problems that need to be addressed when adding GO into the PA layer via IP method. In terms of method, IP process which involves the use of rubber roller to remove excess amine monomers prior to introducing acyl chloride monomers often leads to uneven distribution and/or significant loss of GO from the substrate surface (Lai *et al.*, 2019), especially when GO is weakly adhered to the substrate (Lim *et al.*, 2020). In terms of nanofillers, large lateral size of GO could affect PA integrity by obstructing the diffusion of amine to the organic phase and its incomplete accommodation within the PA layer. As reported by Akther *et al.* (2020), GO with average area of $1.06 \mu\text{m}^2$ or lateral size $<5 \mu\text{m}$ could lead to defective PA layer. Despite being atom-level thick, the large lateral size of GO makes it difficult to be completely accommodated within the several hundreds of nanometer thick PA (Yin, Zhu and

Deng, 2016; Rodríguez *et al.*, 2020), particularly when these nanosheets are not properly arranged (Lim *et al.*, 2020). Therefore, in the second part of this study, a positively charged polyethyleneimine (PEI) is used as interlayer while the rubber rolling method is replaced with oven-drying method to remove the excess amine monomers. The purpose of using PEI interlayer is to improve the arrangement/orientation and adherence of negatively charged GO via electrostatic interaction while the adoption of oven-drying method is to minimize uneven distribution of GO on substrate surface. Interlayer-assisted IP is an emerging technique that could precisely control the polymerization process to produce thin and defect-free PA layer. This technique has been demonstrated for the fabrication of nanofiltration (NF) and forward osmosis (FO) membranes, but its potential use for RO membrane fabrication is yet to be documented. It is anticipated that TFN membranes with enhanced PA integrity, by minimizing defects formation, could be generated via the PEI-interlayered assisted IP.

Loading is another important factor when adding GO into the PA layer. Even though GO exhibits good dispersity in aqueous or polar solvents, excessive amount of GO can still lead to agglomeration. GO agglomeration or aggregation is undesired because it could lead to the formation of non-selective interfacial voids that adversely affects the separation performances of membrane. To date, numerous studies were conducted to investigate the effects of GO loading on the properties and performances of TFN membrane (He *et al.*, 2015; Yin, Zhu and Deng, 2016; Ali *et al.*, 2016) but not for interlayered TFN membrane. Alignment of GO induced by PEI could possibly affect the maximum amount of GO that could be accommodated within the PA layer. Thus, the third part of this study will investigate the effects of GO loading on the properties and performances of PEI-interlayered TFN membrane. In addition, the change in GO position due to the presence of PEI interlayer could possibly affect its positive features. Thus, the performances of PEI-interlayered TFN membrane with respect to chlorine resistivity, antifouling and antibacterial property will be evaluated at the last part of this study.

1.3 Research Objectives

Based on the research problems highlighted in the previous sub-section, the following objectives are set out:

1. To investigate the effects of post IP rinsing on the physicochemical properties and filtration performances of TFC RO membrane by varying the types of rinsing solution and rinsing conditions.
2. To investigate the impacts of PEI interlayer on the physicochemical properties and filtration performances of TFN RO membrane by depositing the PEI on the surface of polysulfone (PSf) substrate at different coating parameters.
3. To investigate the effects of GO on the physicochemical properties and filtration performances of PEI-interlayered TFN RO membrane by incorporating different GO loadings into the PA layer.
4. To evaluate the performances of selected PEI-interlayered TFN RO membrane with respect to chlorine resistivity, antifouling and antibacterial properties.

1.4 Research Scopes

In order to achieve the objectives of this research, the following scopes are planned:

For Objective 1:

- (a) Fabricating TFC RO membranes via IP using rubber rolling technique (aqueous phase: 2 wt/v% m-phenylenediamine (MPD); organic phase: 0.1 wt/v% trimesoyl chloride (TMC)). The resultant membranes are subjected to post IP rinsing using water and various organic solvents (i.e., hexane, cyclohexane and Isoparaffin-G) at different rinsing conditions (i.e., with rinsing and with post air-drying and rinsing) prior to heat treatment.

- (b) Characterizing surface hydrophilicity, morphology, roughness and functional groups of TFC RO membranes using contact angle goniometer, field emission scanning electron microscopy (FESEM), atomic force microscopy (AFM) and attenuated total reflectance Fourier-transform infrared spectroscopy (ATR-FTIR).
- (c) Estimating membranes pore radii based on irreversible thermodynamic model and Steric Hindrance Pore Model by filtrating 40 mg/L glucose, glycerol and ethylene glycol (EG) at different pressures (i.e., 11, 13, 15 and 17 bar) using dead-end RO filtration system.
- (d) Evaluating the pure water flux (PWF) and sodium chloride (NaCl) rejection of TFC RO membranes fabricated via IP using RO water and 2000 mg/L NaCl, respectively, as feed solution in dead-end RO filtration system.

For Objective 2:

- (a) Synthesizing GO from graphite powder using modified Hummers' method.
- (b) Characterizing the physicochemical properties of self-synthesized GO using transmission electron microscopy (TEM), AFM, FTIR, Ultraviolet-visible (UV-vis) spectrophotometry and X-ray diffraction (XRD) spectroscopy.
- (c) Modifying PSf substrate using PEI solution by varying several coating parameters (i.e., concentration (0.005–0.2 wt/v%), drying time (0–120 min) and coating layer number (1–3 layers)).
- (d) Characterizing surface hydrophilicity, morphology, roughness, charge and functional groups of PEI-coated PSf substrates using contact angle goniometer, FESEM, AFM, zeta potential analyzer and ATR-FTIR.
- (e) Determining PEI-coated PSf substrates molecular weight cut-off (MWCO) by filtrating 100 mg/L polyethylene glycol (PEG) with different molecular weight (MW) (i.e., 600, 3400, 8000, 10,000 and 12,000 g/mol) using dead-end RO filtration system.
- (f) Fabricating TFN RO membranes via IP and interlayer-assisted IP using oven-drying technique (aqueous phase: 2 wt/v% MPD and 0.015wt/v% GO; organic phase: 0.1 wt/v% TMC). The resultant membrane is subjected to post IP rinsing

using the best rinsing solution and condition discovered from Objective 1 prior to heat treatment.

- (g) Characterizing surface hydrophilicity, morphology, roughness, and functional groups of TFN RO membranes using contact angle goniometer, TEM, FESEM, AFM and ATR-FTIR.
- (h) Evaluating the pure water permeability (PWP) and NaCl rejection of TFN RO membranes fabricated via IP and interlayer-assisted IP using RO water and 2000 mg/L NaCl, respectively, as feed solution in dead-end RO filtration system.

For Objective 3:

- (a) Fabricating TFC RO membrane via IP using oven-drying technique (aqueous phase: 2 wt/v% MPD; organic phase: 0.1 wt/v% TMC). The resultant membrane is subjected to post IP rinsing using the best rinsing solution and condition discovered from Objective 1 prior to heat treatment.
- (b) Fabricating TFC and TFN RO membranes via interlayer-assisted IP using oven-drying technique (aqueous phase: 2 wt/v% MPD and 0–0.02wt/v% GO; organic phase: 0.1 wt/v% TMC). The resultant membrane is subjected to post IP rinsing using the best rinsing solution and condition discovered from Objective 1 prior to heat treatment.
- (c) Characterizing surface hydrophilicity, morphology, roughness, charge and functional groups of TFN RO membranes using contact angle goniometer, FESEM, AFM, zeta potential analyzer, ATR-FTIR and X-ray photoelectron spectroscopy (XPS).
- (d) Evaluating the PWP and NaCl rejection of TFC and TFN RO membranes fabricated via IP and interlayer-assisted IP using RO water and 2000 mg/L NaCl, respectively, as feed solution in dead-end RO filtration system.

For Objective 4:

- (a) Comparing chlorine resistivity of TFC with optimized TFN RO membrane fabricated via interlayer-assisted IP by exposing the membranes to different concentrations of sodium hypochlorite (NaOCl) (i.e., 500 and 1000 mg/L).
- (b) Comparing antifouling property of TFC with optimized TFN RO membrane fabricated via interlayer-assisted IP using a mixture of 1000 mg/L sodium alginate (NaAlg) with 2000 mg/L NaCl as feed solution.
- (c) Comparing antibacterial property of TFC with optimized TFN RO membrane fabricated via interlayer-assisted IP using two different types of bacteria (i.e., gram-negative *Escherichia Coli* (*E. coli*) and gram-positive *Staphylococcus aureus* (*S. aureus*)).

1.5 Significance of Study

Over the past decade, TFN membrane acted as one of the most promising strategies to tackle all the limitations of PA TFC membranes. Previous studies showed that the addition of nanofillers, particularly GO, into the PA layer mostly focused on overcoming the membrane permeability and selectivity trade-off, chlorine sensitivity and fouling propensity (Chae *et al.*, 2015; He *et al.*, 2015; Yin, Zhu and Deng, 2016; Ali *et al.*, 2016; Inurria *et al.*, 2019). Little attention was paid on the effects of GO deposition on PA integrity and thus the membrane performances. Referring to some of the previous studies, random arrangement of large GO within the PA layer could affect membrane integrity and jeopardize its selectivity (Lim *et al.*, 2020; Rodríguez *et al.*, 2020). Significant loss and/or poor distribution of GO within the PA layer could reduce the positive features of GO in the synthesized TFN membrane (Lai *et al.*, 2016b, 2019).

This study aims to pioneer the production of GO incorporated TFN membrane with improved arrangement/orientation and optimized loading that paves ways to the better PA integrity via interlayer-assisted IP technique. The use of interlayer for the fabrication of NF and FO membranes are common but not for RO membrane.

Introducing interlayer as demonstrated in this work is able to improve the deposition of nanofillers in the RO membrane, improving the membrane water permeability without significantly compromising its selectivity. The findings of this work also provides an in-depth insight to the effects of GO position on membrane physicochemical properties and their ultimate performances on membrane chlorine resistivity, antifouling and antibacterial property. This could prevent membrane researchers from stumble upon the same issue and speed up the development of membrane for saline water desalination in the future. The outcomes of the study clearly indicates the potential of interlayer-assisted IP in producing GO-containing TFN membrane with better PA integrity and properties for water desalination.

1.6 Assumptions and Limitations of Study

Due to the flexibility of IP parameters (i.e., monomer types and concentrations, immersion and reaction time, heat treatment conditions and types of organic solvent used), the parameters used for the fabrication of TFC and TFN membranes as reported by Wan Azelee *et al.* (2017) was adopted to narrow down the scope. The incomplete removal of preservatives coated on commercial substrate could possibly affect the formation of PA or the performance of resultant TFC membrane and to narrow down the scope again, the exact preservatives removal procedure that was reported by Chong *et al.* (2018) was followed. The amount of nanofillers deposited within the selective layer was not quantified as it was nearly impossible to isolate the thin PA from the nanofillers. Moreover, it was difficult to distinguish whether the elemental composition of carbon and oxygen in the selective layer and the chemical bonding of O=C=O and C-C analyzed from the high-resolution spectra was contributed by GO or PA since both of them contain these elements and functional groups. The exact chemical interaction between MPD and PEI was unable to be accurately determined since it is not a strong chemical bond like ionic or covalent bond.

REFERENCES

- Abadikhah, H., Naderi Kalali, E., Khodi, S., Xu, X. and Agathopoulos, S. (2019) Multifunctional thin-film nanofiltration membrane incorporated with reduced graphene oxide@TiO₂@Ag nanocomposites for high desalination performance, dye retention, and antibacterial properties, *ACS Appl. Mater. Interfaces*, 11(26), 23535–23545.
- Abbaszadeh, M., Krizak, D. and Kundu, S. (2019) Layer-by-layer assembly of graphene oxide nanoplatelets embedded desalination membranes with improved chlorine resistance, *Desalination*, 470, 114116.
- Abdikheibari, S., Lei, W., Dumée, L. F., Milne, N. and Baskaran, K. (2018) Thin film nanocomposite nanofiltration membranes from amine functionalized-boron nitride/polypiperazine amide with enhanced flux and fouling resistance, *J. Mater. Chem. A*, 6(25), 12066–12081.
- Adamczak, M., Kamińska, G. and Bohdziewicz, J. (2019) Preparation of Polymer Membranes by In Situ Interfacial Polymerization, *Int. J. Polym. Sci.*, 2019, 1–13.
- Adetayo, A. and Runsewe, D. (2019) Synthesis and Fabrication of Graphene and Graphene Oxide: A Review, *Open J. Compos. Mater.*, 09(02), 207–229.
- Ahmad, N. A., Goh, P. S., Wong, K. C., Zulhairun, A. K. and Ismail, A. F. (2020) Enhancing desalination performance of thin film composite membrane through layer by layer assembly of oppositely charged titania nanosheet, *Desalination*, 476, 114167.
- Akbari, A., Solymani, H. and Rostami, S. M. M. (2015) Preparation and characterization of a novel positively charged nanofiltration membrane based on polysulfone, *J. Appl. Polym. Sci.*, 132(22), 1–9.
- Akther, N., Yuan, Z., Chen, Y., Lim, S., Phuntsho, S., Ghaffour, N., Matsuyama, H. and Shon, H. (2020) Influence of graphene oxide lateral size on the properties and performances of forward osmosis membrane, *Desalination*, 484, 114421.
- Al-Amoudi, A. and Lovitt, R. W. (2007) Fouling strategies and the cleaning system of NF membranes and factors affecting cleaning efficiency, *J. Membr. Sci.*, 303(1–2), 4–28.

- Ali, A., Tufa, R. A., Macedonio, F., Curcio, E. and Drioli, E. (2018) Membrane technology in renewable-energy-driven desalination, *Renew. Sustain. Energy Rev.*, 81, 1–21.
- Ali, M. E. A., Wang, L., Wang, X. and Feng, X. (2016) Thin film composite membranes embedded with graphene oxide for water desalination, *Desalination*, 386, 67–76.
- Ali, Z., Al Sunbul, Y., Pacheco, F., Ogieglo, W., Wang, Y., Genduso, G. and Pinnau, I. (2019) Defect-free highly selective polyamide thin-film composite membranes for desalination and boron removal, *J. Membr. Sci.*, 578, 85–94.
- Anastacio-López, Z. S., Gonzalez-Calderon, J. A., Saldivar-Guerrero, R., Velasco-Santos, C., Martínez-Hernández, A. L., Fierro-González, J. C. and Almendárez-Camarillo, A. (2019) Modification of graphene oxide to induce beta crystals in isotactic polypropylene, *J. Mater. Sci.*, 54(1), 427–443.
- Armendáriz-Ontiveros, M. M., García García, A., de los Santos Villalobos, S. and Fimbres Weihs, G. A. (2019) Biofouling performance of RO membranes coated with Iron NPs on graphene oxide, *Desalination*, 451, 45–58.
- Asempour, F., Akbari, S., Bai, D., Emadzadeh, D., Matsuura, T. and Kruczek, B. (2018a) Improvement of stability and performance of functionalized halloysite nano tubes-based thin film nanocomposite membranes, *J. Membr. Sci.*, 563, 470–480.
- Asempour, F., Emadzadeh, D., Matsuura, T. and Kruczek, B. (2018b) Synthesis and characterization of novel Cellulose Nanocrystals-based Thin Film Nanocomposite membranes for reverse osmosis applications, *Desalination*, 439, 179–187.
- Ba, C., Langer, J. and Economy, J. (2009) Chemical modification of P84 copolyimide membranes by polyethylenimine for nanofiltration, *J. Membr. Sci.*, 327(1–2), 49–58.
- Badalov, S., Oren, Y. and Arnusch, C. J. (2015) Ink-jet printing assisted fabrication of patterned thin film composite membranes, *J. Membr. Sci.*, 493(June 2015), 508–514.
- Baek, Y., Kim, H. J., Kim, S.-H., Lee, J.-C. and Yoon, J. (2017) Evaluation of carbon nanotube-polyamide thin-film nanocomposite reverse osmosis membrane: Surface properties, performance characteristics and fouling behavior, *J. Ind. Eng. Chem.*, 56, 327–334.

- Bahar, R. and Hawlader, M. N. A. (2013) Desalination: Conversion of Seawater to Freshwater. *2nd International Conference on Mechanical, Automotive and Aerospace Engineering (ICMAAE 2013)*. 2013.
- Baroña, G. N. B., Lim, J., Choi, M. and Jung, B. (2013) Interfacial polymerization of polyamide-aluminosilicate SWNT nanocomposite membranes for reverse osmosis, *Desalination*, 325, 138–147.
- Ben-Sasson, M., Lu, X., Bar-Zeev, E., Zodrow, K. R., Nejati, S., Qi, G., Giannelis, E. P. and Elimelech, M. (2014a) In situ formation of silver nanoparticles on thin-film composite reverse osmosis membranes for biofouling mitigation, *Water Res.*, 62, 260–270.
- Ben-Sasson, M., Lu, X., Nejati, S., Jaramillo, H. and Elimelech, M. (2016) In situ surface functionalization of reverse osmosis membranes with biocidal copper nanoparticles, *Desalination*, 388, 1–8.
- Ben-Sasson, M., Zodrow, K. R., Genggeng, Q., Kang, Y., Giannelis, E. P. and Elimelech, M. (2014b) Surface Functionalization of Thin-Film Composite Membranes with Copper Nanoparticles for Antimicrobial Surface Properties, *Environ. Sci. Technol.*, 48(1), 384–393.
- Bláha, M., Trchová, M., Morávková, Z., Humpolíček, P. and Stejskal, J. (2018) Semiconducting materials from oxidative coupling of phenylenediamines under various acidic conditions, *Mater. Chem. Phys.*, 205, 423–435.
- Blattmann, C. O. and Pratsinis, S. E. (2019) Nanoparticle Filler Content and Shape in Polymer Nanocomposites, *KONA Powder Part. J.*, 36, 3–32.
- Boo, C., Wang, Y., Zucker, I., Choo, Y., Osuji, C. O. and Elimelech, M. (2018) High Performance Nanofiltration Membrane for Effective Removal of Perfluoroalkyl Substances at High Water Recovery, *Environ. Sci. Technol.*, 52(13), 7279–7288.
- Boretti, A. and Rosa, L. (2019) Reassessing the projections of the World Water Development Report, *npj Clean Water*, 2(15), 1–6.
- Bowen, W. R. and Mohammad, A. W. (1998) Characterization and Prediction of Nanofiltration Membrane Performance—A General Assessment, *Chem. Eng. Res. Des.*, 76(8), 885–893.
- Brende, B. (2020) *The Global Risks Report 2020 (15th Edition)*.
- Brisebois, P. P. and Siaj, M. (2020) Harvesting graphene oxide – years 1859 to 2019: a review of its structure, synthesis, properties and exfoliation, *J. Mater. Chem. C*, 8(5), 1517–1547.

- Brodie, B. C. (1859) XIII. On the atomic weight of graphite, *Philos. Trans. R. Soc. London*, 149, 249–259.
- Cadotte, J. E., Cobian, K. E., Forester, R. H. and Petersen, R. J. (1975) *In Situ-Formed Condensation Polymers for Reverse Osmosis Membranes*.
- Cadotte, J. E., Cobian, K. E., Forester, R. H. and Petersen, R. J. (1976) *Continued Evaluation of In Situ-Formed Condensation Polymers for Reverse Osmosis Membranes*.
- Cadotte, J. E., Petersen, R. J., Larson, R. E. and Erickson, E. E. (1980) A new thin-film composite seawater reverse osmosis membrane, *Desalination*, 32, 25–31.
- Cadotte, J. E. and Peterson, R. J. (1981) *Thin-Film Composite Reverse-Osmosis Membranes: Origin, Development, and Recent Advances*. *Synthetic Membranes*. American Chemical Society, 305–326.
- Cay-durgun, P. and Lind, M. L. (2018) Nanoporous materials in polymeric membranes for desalination, *Curr. Opin. Chem. Eng.*, 20, 19–27.
- Chae, H. R., Lee, C. H., Park, P. K., Kim, I. C. and Kim, J. H. (2017) Synergetic effect of graphene oxide nanosheets embedded in the active and support layers on the performance of thin-film composite membranes, *J. Membr. Sci.*, 525, 99–106.
- Chae, H. R., Lee, J., Lee, C. H., Kim, I. C. and Park, P. K. (2015) Graphene oxide-embedded thin-film composite reverse osmosis membrane with high flux, anti-biofouling, and chlorine resistance, *J. Membr. Sci.*, 483, 128–135.
- Chai, G. Y. and Krantz, W. B. (1994) Formation and characterization of polyamide membranes via interfacial polymerization, *J. Membr. Sci.*, 93(2), 175–192.
- Chen, J., Yao, B., Li, C. and Shi, G. (2013) An improved Hummers method for eco-friendly synthesis of graphene oxide, *Carbon N. Y.*, 64(1), 225–229.
- Chiao, Y. H., Sengupta, A., Chen, S. T., Hung, W. S., Lai, J. Y., Upadhyaya, L., Qian, X. and Wickramasinghe, S. R. (2020) Novel thin-film composite forward osmosis membrane using polyethylenimine and its impact on membrane performance, *Sep. Sci. Technol.*, 55(3), 590–600.
- Choi, H. G., Shah, A. A., Nam, S. E., Park, Y. I. and Park, H. (2019) Thin-film composite membranes comprising ultrathin hydrophilic polydopamine interlayer with graphene oxide for forward osmosis, *Desalination*, 449, 41–49.
- Choi, W., Choi, J., Bang, J. and Lee, J. H. (2013) Layer-by-Layer Assembly of Graphene Oxide Nanosheets on Polyamide Membranes for Durable Reverse-Osmosis Applications, *ACS Appl. Mater. Interfaces*, 5(23), 12510–12519.

- Choi, W., Jeon, S., Kwon, S. J., Park, H., Park, Y. I., Nam, S. E., Lee, P. S., Lee, J. S., Choi, J., Hong, S., Chan, E. P. and Lee, J. H. (2017) Thin film composite reverse osmosis membranes prepared via layered interfacial polymerization, *J. Membr. Sci.*, 527, 121–128.
- Chong, C. Y., Lau, W. J., Yusof, N., Lai, G. S. and Ismail, A. F. (2019) Roles of nanomaterial structure and surface coating on thin film nanocomposite membranes for enhanced desalination, *Compos. Part B Eng.*, 160, 471–479.
- Chong, C. Y., Lau, W. J., Yusof, N., Lai, G. S., Othman, N. H., Matsuura, T. and Ismail, A. F. (2018) Studies on the properties of RO membranes for salt and boron removal: Influence of thermal treatment methods and rinsing treatments, *Desalination*, 428, 218–226.
- Chua, C. K. and Pumera, M. (2014) Chemical reduction of graphene oxide: a synthetic chemistry viewpoint, *Chem. Soc. Rev.*, 43(1), 291–312.
- Cosgrove, W. and Rijsberman, F. (2000) *World Water Vision: Making Water Everybody's Business. Climate Change 2013 - The Physical Science Basis*. London, UK: Earthscan Publications Ltd.
- Cui, Y., Liu, X. Y. and Chung, T. S. (2017) Ultrathin Polyamide Membranes Fabricated from Free-Standing Interfacial Polymerization: Synthesis, Modifications, and Post-treatment, *Ind. Eng. Chem. Res.*, 56(2), 513–523.
- Dai, R., Li, J. and Wang, Z. (2020) Constructing interlayer to tailor structure and performance of thin-film composite polyamide membranes: A review, *Adv. Colloid Interface Sci.*, 282, 102204.
- David R Lide (2003) *Handbook of Chemistry and Physics, 84th Edition*. LLC:Boca Raton: CRC Press.
- Dimiev, A. M. (2016) *Mechanism of Formation and Chemical Structure of Graphene Oxide. Graphene Oxide: Fundamentals and Applications*. Chichester, UK: John Wiley & Sons, Ltd, 36–84.
- Ding, W., Li, Y., Bao, M., Zhang, J., Zhang, C. and Lu, J. (2017) Highly permeable and stable forward osmosis (FO) membrane based on the incorporation of Al₂O₃ nanoparticles into both substrate and polyamide active layer, *RSC Adv.*, 7(64), 40311–40320.
- Dlamini, D. S., Mamba, B. B. and Li, J. (2019) The role of nanoparticles in the performance of nano-enabled composite membranes – A critical scientific perspective, *Sci. Total Environ.*, 656, 723–731.

- Dong, H., Wu, L., Zhang, L., Chen, H. and Gao, C. (2015) Clay nanosheets as charged filler materials for high-performance and fouling-resistant thin film nanocomposite membranes, *J. Membr. Sci.*, 494, 92–103.
- Dreyer, D. R., Park, S., Bielawski, C. W. and Ruoff, R. S. (2010) The chemistry of graphene oxide, *Chem. Soc. Rev.*, 39(1), 228–240.
- El-Aassar, A. hameed M. A. (2012) Polyamide thin film composite membranes using interfacial polymerization: Synthesis, characterization and reverse osmosis performance for water desalination, *Aust. J. Basic Appl. Sci.*, 6(6), 382–391.
- El-Aassar, A. M. A. (2014) Improvement of reverse osmosis performance of polyamide thin-film composite membranes using TiO₂ nanoparticles, *Desalin. Water Treat.*, 55(11), 1–12.
- El-Arnaouty, M. B., Abdel Ghaffar, A. M., Eid, M., Aboulfotouh, M. E., Taher, N. H. and Soliman, E.-S. (2018) Nano-modification of polyamide thin film composite reverse osmosis membranes by radiation grafting, *J. Radiat. Res. Appl. Sci.*, 11(3), 204–216.
- Elsaid, K., Sayed, E. T., Abdelkareem, M. A., Mahmoud, M. S., Ramadan, M. and Olabi, A. G. (2020) Environmental impact of emerging desalination technologies: A preliminary evaluation, *J. Environ. Chem. Eng.*, 8(5), 104099.
- Emadzadeh, D., Ghanbari, M., Lau, W. J., Rahbari-Sisakht, M., Rana, D., Matsuura, T., Kruczek, B. and Ismail, A. F. (2017) Surface modification of thin film composite membrane by nanoporous titanate nanoparticles for improving combined organic and inorganic antifouling properties, *Mater. Sci. Eng. C*, 75, 463–470.
- Emadzadeh, D., Lau, W. J., Rahbari-Sisakht, M., Daneshfar, A., Ghanbari, M., Mayahi, A., Matsuura, T. and Ismail, A. F. (2015) A novel thin film nanocomposite reverse osmosis membrane with superior anti-organic fouling affinity for water desalination, *Desalination*, 368, 106–113.
- Farahbakhsh, J., Delnavaz, M. and Vatanpour, V. (2019) Simulation and characterization of novel reverse osmosis membrane prepared by blending polypyrrole coated multiwalled carbon nanotubes for brackish water desalination and antifouling properties using artificial neural networks, *J. Membr. Sci.*, 581, 123–138.

- Farahbaksh, J., Delnavaz, M. and Vatanpour, V. (2017) Investigation of raw and oxidized multiwalled carbon nanotubes in fabrication of reverse osmosis polyamide membranes for improvement in desalination and antifouling properties, *Desalination*, 410, 1–9.
- Fathizadeh, M., Aroujalian, A. and Raisi, A. (2015) Preparation and characterization of thin film composite reverse osmosis membranes with wet and dry support layer, *Desalin. Water Treat.*, 56(9), 2284–2295.
- Feng, C., Xu, J., Li, M., Tang, Y. and Gao, C. (2014) Studies on a novel nanofiltration membrane prepared by cross-linking of polyethyleneimine on polyacrylonitrile substrate, *J. Membr. Sci.*, 451, 103–110.
- Fraga, T. J. M., Carvalho, M. N., Ghislandi, M. G. and Motta Sobrinho, M. A. da (2019) Functionalized graphene-based materials as innovative adsorbents of organic pollutants: A concise overview, *Brazilian J. Chem. Eng.*, 36(1), 1–31.
- Frankberg, E. J., George, L., Efimov, A., Honkanen, M., Pessi, J. and Levänen, E. (2015) Measuring synthesis yield in graphene oxide synthesis by modified Hummers method, *Fullerenes, Nanotub. Carbon Nanostructures*, 23(9), 755–759.
- Freger, V. (2003) Nanoscale heterogeneity of polyamide membranes formed by interfacial polymerization, *Langmuir*, 19(11), 4791–4797.
- Freger, V. (2005) Kinetics of film formation by interfacial polycondensation, *Langmuir*, 21(5), 1884–1894.
- Freger, V. and Srebnik, S. (2003) Mathematical model of charge and density distributions in interfacial polymerization of thin films, *J. Appl. Polym. Sci.*, 88(5), 1162–1169.
- Gao, X., Li, Y., Yang, X., Shang, Y., Wang, Y., Gao, B. and Wang, Z. (2017) Highly permeable and antifouling reverse osmosis membranes with acidified graphitic carbon nitride nanosheets as nanofillers, *J. Mater. Chem. A*, 5(37), 19875–19883.
- García, A., Rodríguez, B., Oztürk, D., Rosales, M., Diaz, D. I. and Mautner, A. (2018) Incorporation of CuO nanoparticles into thin-film composite reverse osmosis membranes (TFC-RO) for antibiofouling properties, *Polym. Bull.*, 75(5), 2053–2069.

- Ghanbari, M., Emadzadeh, D., Lau, W. J., Matsuura, T. and Ismail, A. F. (2015) Synthesis and characterization of novel thin film nanocomposite reverse osmosis membranes with improved organic fouling properties for water desalination, *RSC Adv.*, 5(27), 21268–21276.
- Gholami, M., Nasser, S., Feng, C. Y., Matsuura, T. and Khulbe, K. C. (2003) The effect of heat-treatment on the ultrafiltration performance of polyethersulfone (PES) hollow-fiber membranes, *Desalination*, 155(3), 293–301.
- Ghosh, A. K. and Bindal, R. C. (2017) Impacts of heat treatment medium on performance of aliphatic-aromatic and aromatic-aromatic based thin-film composite (TFC) polyamide reverse osmosis (RO) membrane, *J. Polym. Mater.*, 34(4), 759–772.
- Ghosh, A. K. and Hoek, E. M. V. (2009) Impacts of support membrane structure and chemistry on polyamide–polysulfone interfacial composite membranes, *J. Membr. Sci.*, 336(1–2), 140–148.
- Ghosh, A. K., Jeong, B. H., Huang, X. and Hoek, E. M. V. (2008) Impacts of reaction and curing conditions on polyamide composite reverse osmosis membrane properties, *J. Membr. Sci.*, 311(1–2), 34–45.
- Goh, P. S., Lau, W. J., Othman, M. H. D. and Ismail, A. F. (2018) Membrane fouling in desalination and its mitigation strategies, *Desalination*, 425, 130–155.
- Goh, P. S., Matsuura, T., Ismail, A. F. and Hilal, N. (2016) Recent trends in membranes and membrane processes for desalination, *Desalination*, 391, 43–60.
- Greenlee, L. F., Lawler, D. F., Freeman, B. D., Marrot, B. and Moulin, P. (2009) Reverse osmosis desalination: Water sources, technology, and today's challenges, *Water Res.*, 43(9), 2317–2348.
- Gu, J. E., Lee, S., Stafford, C. M., Lee, J. S., Choi, W., Kim, B. Y., Baek, K. Y., Chan, E. P., Chung, J. Y., Bang, J. and Lee, J. H. (2013) Molecular Layer-by-Layer Assembled Thin-Film Composite Membranes for Water Desalination, *Adv. Mater.*, 25(34), 4778–4782.
- Gu, L., Xie, M.-Y., Jin, Y., He, M., Xing, X.-Y., Yu, Y. and Wu, Q.-Y. (2019) Construction of Antifouling Membrane Surfaces through Layer-by-Layer Self-Assembly of Lignosulfonate and Polyethyleneimine, *Polymers (Basel)*, 11(11), 1782.

- Gullinkala, T., Digman, B., Gorey, C., Hausman, R. and Escobar, I. C. (2010) *Chapter 4 Desalination: Reverse Osmosis and Membrane Distillation. Sustainability Science and Engineering*. Elsevier, 65–93.
- Hailemariam, R. H., Woo, Y. C., Damtie, M. M., Kim, B. C., Park, K. D. and Choi, J. S. (2020) Reverse osmosis membrane fabrication and modification technologies and future trends: A review, *Adv. Colloid Interface Sci.*, 276, 102100.
- Halakoo, E. and Feng, X. (2020) Layer-by-layer assembly of polyethyleneimine/graphene oxide membranes for desalination of high-salinity water via pervaporation, *Sep. Purif. Technol.*, 234, 116077.
- He, H., Klinowski, J., Forster, M. and Lerf, A. (1998) A new structural model for graphite oxide, *Chem. Phys. Lett.*, 287(1–2), 53–56.
- He, L., Dumée, L. F., Feng, C., Velleman, L., Reis, R., She, F., Gao, W. and Kong, L. (2015) Promoted water transport across graphene oxide–poly(amide) thin film composite membranes and their antibacterial activity, *Desalination*, 365, 126–135.
- Hegab, H. M. and Zou, L. (2015) Graphene oxide-assisted membranes: Fabrication and potential applications in desalination and water purification, *J. Membr. Sci.*, 484, 95–106.
- Hermans, S., Bernstein, R., Volodin, A. and Vankelecom, I. F. J. (2015) Study of synthesis parameters and active layer morphology of interfacially polymerized polyamide–polysulfone membranes, *React. Funct. Polym.*, 86, 199–208.
- Hermans, S., Mariën, H., Dom, E., Bernstein, R. and Vankelecom, I. F. J. (2014) Simplified synthesis route for interfacially polymerized polyamide membranes, *J. Membr. Sci.*, 451, 148–156.
- Holycross, D. R. and Chai, M. (2013) Comprehensive NMR Studies of the Structures and Properties of PEI Polymers, *Macromolecules*, 46(17), 6891–6897.
- Huang, F. L., Wang, Q. Q., Wei, Q. F., Gao, W. D., Shou, H. Y. and Jiang, S. D. (2010) Dynamic wettability and contact angles of poly(vinylidene fluoride) nanofiber membranes grafted with acrylic acid, *Express Polym. Lett.*, 4(9), 551–558.
- Huang, H., Qu, X., Dong, H., Zhang, L. and Chen, H. (2013a) Role of NaA zeolites in the interfacial polymerization process towards a polyamide nanocomposite reverse osmosis membrane, *RSC Adv.*, 3(22), 8203–8207.

- Huang, H., Qu, X., Ji, X., Gao, X., Zhang, L., Chen, H. and Hou, L. (2013b) Acid and multivalent ion resistance of thin film nanocomposite RO membranes loaded with silicalite-1 nanozeolites, *J. Mater. Chem. A*, 1(37), 11343–11349.
- Huang, H., Ying, Y. and Peng, X. (2014) Graphene oxide nanosheet: an emerging star material for novel separation membranes, *J. Mater. Chem. A*, 2(34), 13772–13782.
- Hummers, W. S. and Offeman, R. E. (1958) Preparation of Graphitic Oxide, *J. Am. Chem. Soc.*, 80(6), 1339–1339.
- Idris, A. and Mat Zain, N. (2006) Effect of heat treatment on the performance and structural details of polyethersulfone ultrafiltration membranes, *J. Teknol.*, 44(1), 27–40.
- Inukai, S., Cruz-Silva, R., Ortiz-Medina, J., Morelos-Gomez, A., Takeuchi, K., Hayashi, T., Tanioka, A., Araki, T., Tejima, S., Noguchi, T., Terrones, M. and Endo, M. (2015) High-performance multi-functional reverse osmosis membranes obtained by carbon nanotube-polyamide nanocomposite, *Sci. Rep.*, 5, 1–10.
- Inurria, A., Cay-Durgun, P., Rice, D., Zhang, H., Seo, D. K., Lind, M. L. and Perreault, F. (2019) Polyamide thin-film nanocomposite membranes with graphene oxide nanosheets: Balancing membrane performance and fouling propensity, *Desalination*, 451, 139–147.
- Isawi, H. (2018) Development of thin-film composite membranes via radical grafting with methacrylic acid/ ZnO doped TiO₂ nanocomposites, *React. Funct. Polym.*, 131(September), 400–413.
- Isawi, H., El-Sayed, M. H., Feng, X., Shawky, H. and Abdel Mottaleb, M. S. (2016) Surface nanostructuring of thin film composite membranes via grafting polymerization and incorporation of ZnO nanoparticles, *Appl. Surf. Sci.*, 385, 268–281.
- Ismail, A. F. and Matsuura, T. (2018) Progress in transport theory and characterization method of Reverse Osmosis (RO) membrane in past fifty years, *Desalination*, 434, 2–11.
- Jegal, J., Min, S. G. and Lee, K. H. (2002) Factors affecting the interfacial polymerization of polyamide active layers for the formation of polyamide composite membranes, *J. Appl. Polym. Sci.*, 86(11), 2781–2787.

- Jeong, B. H., Hoek, E. M. V., Yan, Y., Subramani, A., Huang, X., Hurwitz, G., Ghosh, A. K. and Jawor, A. (2007) Interfacial polymerization of thin film nanocomposites: A new concept for reverse osmosis membranes, *J. Membr. Sci.*, 294(1–2), 1–7.
- Jiang, S., Li, Y. and Ladewig, B. P. (2017) A review of reverse osmosis membrane fouling and control strategies, *Sci. Total Environ.*, 595, 567–583.
- Jin, Y., Liang, S., Wu, Z., Cai, Z. and Zhao, N. (2014) Simulating the growth process of aromatic polyamide layer by monomer concentration controlling method, *Appl. Surf. Sci.*, 314, 286–291.
- Jin, Y. and Su, Z. (2009) Effects of polymerization conditions on hydrophilic groups in aromatic polyamide thin films, *J. Membr. Sci.*, 330(1–2), 175–179.
- Jones, E., Qadir, M., van Vliet, M. T. H., Smakhtin, V. and Kang, S. (2019) The state of desalination and brine production: A global outlook, *Sci. Total Environ.*, 657, 1343–1356.
- Kadhom, M. and Deng, B. (2019a) Thin film nanocomposite membranes filled with bentonite nanoparticles for brackish water desalination: A novel water uptake concept, *Microporous Mesoporous Mater.*, 279, 82–91.
- Kadhom, M. and Deng, B. (2019b) Synthesis of high-performance thin film composite (TFC) membranes by controlling the preparation conditions: Technical notes, *J. Water Process Eng.*, 30, 100542.
- Kang, G. and Cao, Y. (2012) Development of antifouling reverse osmosis membranes for water treatment: A review, *Water Res.*, 46(3), 584–600.
- Kang, S., Mauter, M. S. and Elimelech, M. (2009) Microbial cytotoxicity of carbon-based nanomaterials: implications for river water and wastewater effluent, *Environ. Sci. Technol.*, 43(7), 2648–2653.
- Karimi, H., Bazgar Bajestani, M., Mousavi, S. A. and Mokhtari Garakani, R. (2017) Polyamide membrane surface and bulk modification using humid environment as a new heat curing medium, *J. Membr. Sci.*, 523, 129–137.
- Karkhanechi, H., Razi, F., Sawada, I., Takagi, R., Ohmukai, Y. and Matsuyama, H. (2013a) Improvement of antibiofouling performance of a reverse osmosis membrane through biocide release and adhesion resistance, *Sep. Purif. Technol.*, 105, 106–113.

- Karkhanechi, H., Takagi, R., Ohmukai, Y. and Matsuyama, H. (2013b) Enhancing the antibiofouling performance of RO membranes using $\text{Cu}(\text{OH})_2$ as an antibacterial agent, *Desalination*, 325, 40–47.
- Kavitha, J., Rajalakshmi, M., Phani, A. R. and Padaki, M. (2019) Pretreatment processes for seawater reverse osmosis desalination systems—A review, *J. Water Process Eng.*, 32, 100926.
- Kawaguchi, T., Minematsu, H., Hayashi, Y., Hara, S. and Ueda, F. (1982) from <https://patents.google.com/patent/US4360434A/en?q=4%2C360%2C434>.
- Khorshidi, B., Biswas, I., Ghosh, T., Thundat, T. and Sadrzadeh, M. (2018) Robust fabrication of thin film polyamide-TiO₂ nanocomposite membranes with enhanced thermal stability and anti-biofouling propensity, *Sci. Rep.*, 8(1), 784.
- Khorshidi, B., Thundat, T., Fleck, B. A. and Sadrzadeh, M. (2015) Thin film composite polyamide membranes: parametric study on the influence of synthesis conditions, *RSC Adv.*, 5(68), 54985–54997.
- Khorshidi, B., Thundat, T., Fleck, B. A. and Sadrzadeh, M. (2016) A Novel Approach Toward Fabrication of High Performance Thin Film Composite Polyamide Membranes, *Sci. Rep.*, 6(1), 22069.
- Khulbe, K. C. and Matsuura, T. (2017) Recent progresses in preparation and characterization of RO membranes, *J. Membr. Sci. Res.*, 3(3), 174–186.
- Kim, H. J., Choi, K., Baek, Y., Kim, D. G., Shim, J., Yoon, J. and Lee, J. C. (2014) High-performance reverse osmosis CNT/polyamide nanocomposite membrane by controlled interfacial interactions, *ACS Appl. Mater. Interfaces*, 6(4), 2819–2829.
- Kim, H. J., Choi, Y. S., Lim, M. Y., Jung, K. H., Kim, D. G., Kim, J. J., Kang, H. and Lee, J. C. (2016) Reverse osmosis nanocomposite membranes containing graphene oxides coated by tannic acid with chlorine-tolerant and antimicrobial properties, *J. Membr. Sci.*, 514, 25–34.
- Kim, H. J., Lim, M.-Y., Jung, K. H., Kim, D.-G. and Lee, J.-C. (2015) High-performance reverse osmosis nanocomposite membranes containing the mixture of carbon nanotubes and graphene oxides, *J. Mater. Chem. A*, 3(13), 6798–6809.
- Kim, I. C., Jeong, B. R., Kim, S. J. and Lee, K. H. (2013a) Preparation of high flux thin film composite polyamide membrane: The effect of alkyl phosphate additives during interfacial polymerization, *Desalination*, 308, 111–114.

- Kim, S. G., Chun, J. H., Chun, B. H. and Kim, S. H. (2013b) Preparation, characterization and performance of poly(arylene ether sulfone)/modified silica nanocomposite reverse osmosis membrane for seawater desalination, *Desalination*, 325, 76–83.
- Kochan, J., Wintgens, T., Melin, T. and Wong, J. E. (2009) Characterization and filtration performance of coating-modified polymeric membranes used in membrane bioreactors, *Chem. Pap.*, 63(2), 152–157.
- Kochkodan, V. and Hilal, N. (2015) A comprehensive review on surface modified polymer membranes for biofouling mitigation, *Desalination*, 356, 187–207.
- Koroneos, C., Nanaki, E., Moustakas, K. and Malamis, D. (2012) *Renewable Energy Desalination. Renewable Energy Desalination*. The World Bank.
- Kress, N., Gertner, Y. and Shoham-Frider, E. (2020) Seawater quality at the brine discharge site from two mega size seawater reverse osmosis desalination plants in Israel (Eastern Mediterranean), *Water Res.*, 171, 115402.
- Krishnamoorthy, K., Veerapandian, M., Yun, K. and Kim, S. J. (2013) The chemical and structural analysis of graphene oxide with different degrees of oxidation, *Carbon N. Y.*, 53, 38–49.
- Kwon, Y.-N. and Leckie, J. O. (2006) Hypochlorite degradation of crosslinked polyamide membranes II. Changes in hydrogen bonding behavior and performance, *J. Membr. Sci.*, 282(1–2), 456–464.
- Lai, G. S., Lau, W. J., Goh, P. S., Ismail, A. F., Tan, Y. H., Chong, C. Y., Krause-Rehberg, R. and Awad, S. (2018) Tailor-made thin film nanocomposite membrane incorporated with graphene oxide using novel interfacial polymerization technique for enhanced water separation, *Chem. Eng. J.*, 344, 524–534.
- Lai, G. S., Lau, W. J., Goh, P. S., Ismail, A. F., Yusof, N. and Tan, Y. H. (2016a) Graphene oxide incorporated thin film nanocomposite nanofiltration membrane for enhanced salt removal performance, *Desalination*, 387, 14–24.
- Lai, G. S., Lau, W. J., Goh, P. S., Tan, Y. H., Ng, B. C. and Ismail, A. F. (2019) A novel interfacial polymerization approach towards synthesis of graphene oxide-incorporated thin film nanocomposite membrane with improved surface properties, *Arab. J. Chem.*, 12(1), 75–87.

- Lai, G. S., Lau, W. J., Gray, S. R., Matsuura, T., Gohari, R. J., Subramanian, M. N., Lai, S. O., Ong, C. S., Ismail, A. F., Emazadah, D. and Ghanbari, M. (2016b) A practical approach to synthesize polyamide thin film nanocomposite (TFN) membranes with improved separation properties for water/wastewater treatment, *J. Mater. Chem. A*, 4(11), 4134–4144.
- Lattemann, S., Kennedy, M. D., Schippers, J. C. and Amy, G. (2010) *Global Desalination Situation. Sustainability Science and Engineering*. Elsevier, 7–39.
- Lau, W. J., Gray, S., Matsuura, T., Emadzadeh, D., Paul Chen, J. and Ismail, A. F. (2015) A review on polyamide thin film nanocomposite (TFN) membranes: History, applications, challenges and approaches, *Water Res.*, 80, 306–324.
- Lau, W. J. and Ismail, A. F. (2009) Theoretical studies on the morphological and electrical properties of blended PES/SPEEK nanofiltration membranes using different sulfonation degree of SPEEK, *J. Membr. Sci.*, 334(1–2), 30–42.
- Lee, J., Hill, A. and Kentish, S. (2013) Formation of a thick aromatic polyamide membrane by interfacial polymerisation, *Sep. Purif. Technol.*, 104, 276–283.
- Lee, K. P., Arnot, T. C. and Mattia, D. (2011) A review of reverse osmosis membrane materials for desalination — Development to date and future potential, *J. Membr. Sci.*, 370(1–2), 1–22.
- Lee, S. and Elimelech, M. (2006) Relating Organic Fouling of Reverse Osmosis Membranes to Intermolecular Adhesion Forces, *Environ. Sci. Technol.*, 40(3), 980–987.
- Lee, T. H., Oh, J. Y., Hong, S. P., Lee, J. M., Roh, S. M., Kim, S. H. and Park, H. B. (2019) ZIF-8 particle size effects on reverse osmosis performance of polyamide thin-film nanocomposite membranes: Importance of particle deposition, *J. Membr. Sci.*, 570–571, 23–33.
- Li, C., Guan, Z., Liu, D. and Raetz, C. R. H. (2011) Pathway for lipid A biosynthesis in *Arabidopsis thaliana* resembling that of *Escherichia coli*, *Proc. Natl. Acad. Sci. U. S. A.*, 108(28), 11387–11392.
- Li, D., Yan, Y. and Wang, H. (2016) Recent advances in polymer and polymer composite membranes for reverse and forward osmosis processes, *Prog. Polym. Sci.*, 61, 104–155.
- Li, L., Zhang, S., Zhang, X. and Zheng, G. (2008) Polyamide thin film composite membranes prepared from isomeric biphenyl tetraacyl chloride and *m*-phenylenediamine, *J. Membr. Sci.*, 315(1–2), 20–27.

- Li, N., Yu, L., Xiao, Z., Jiang, C., Gao, B. and Wang, Z. (2020) Biofouling mitigation effect of thin film nanocomposite membranes immobilized with laponite mediated metal ions, *Desalination*, 473, 114162.
- Li, P., Wang, Z., Yang, L., Zhao, S., Song, P. and Khan, B. (2018) A novel loose-NF membrane based on the phosphorylation and cross-linking of polyethyleneimine layer on porous PAN UF membranes, *J. Membr. Sci.*, 555, 56–68.
- Li, S., Gao, B., Wang, Y., Jin, B., Yue, Q. and Wang, Z. (2019a) Antibacterial thin film nanocomposite reverse osmosis membrane by doping silver phosphate loaded graphene oxide quantum dots in polyamide layer, *Desalination*, 464, 94–104.
- Li, Y., Li, C., Li, S., Su, B., Han, L. and Mandal, B. (2019b) Graphene oxide (GO)-interlayered thin-film nanocomposite (TFN) membranes with high solvent resistance for organic solvent nanofiltration (OSN), *J. Mater. Chem. A*, 7(21), 13315–13330.
- Li, Y., Li, S. and Zhang, K. (2017) Influence of hydrophilic carbon dots on polyamide thin film nanocomposite reverse osmosis membranes, *J. Membr. Sci.*, 537, 42–53.
- Li, Y., Yang, S., Zhang, K. and Van der Bruggen, B. (2019c) Thin film nanocomposite reverse osmosis membrane modified by two dimensional laminar MoS₂ with improved desalination performance and fouling-resistant characteristics, *Desalination*, 454, 48–58.
- Liang, Y., Li, C., Li, S., Su, B., Hu, M. Z., Gao, X. and Gao, C. (2020) Graphene quantum dots (GQDs)-polyethyleneimine as interlayer for the fabrication of high performance organic solvent nanofiltration (OSN) membranes, *Chem. Eng. J.*, 380, 122462.
- Lim, S., Park, K. H., Tran, V. H., Akther, N., Phuntsho, S., Choi, J. Y. and Shon, H. K. (2020) Size-controlled graphene oxide for highly permeable and fouling-resistant outer-selective hollow fiber thin-film composite membranes for forward osmosis, *J. Membr. Sci.*, 609, 118171.
- Liu, F., Wang, L., Li, D., Liu, Q. and Deng, B. (2019a) A review: the effect of the microporous support during interfacial polymerization on the morphology and performances of a thin film composite membrane for liquid purification, *RSC Adv.*, 9(61), 35417–35428.

- Liu, L., Xie, X., Qi, S., Li, R., Zhang, X., Song, X. and Gao, C. (2019b) Thin film nanocomposite reverse osmosis membrane incorporated with UiO-66 nanoparticles for enhanced boron removal, *J. Membr. Sci.*, 580, 101–109.
- Liu, L., Zhu, G., Liu, Z. and Gao, C. (2016) Effect of MCM-48 nanoparticles on the performance of thin film nanocomposite membranes for reverse osmosis application, *Desalination*, 394, 72–82.
- Liu, M., Wu, D., Yu, S. and Gao, C. (2009) Influence of the polyacryl chloride structure on the reverse osmosis performance, surface properties and chlorine stability of the thin-film composite polyamide membranes, *J. Membr. Sci.*, 326(1), 205–214.
- Liu, Q. and Xu, G.-R. (2016) Graphene oxide (GO) as functional material in tailoring polyamide thin film composite (PA-TFC) reverse osmosis (RO) membranes, *Desalination*, 394, 162–175.
- Liu, S., Low, Z.-X., Hegab, H. M., Xie, Z., Ou, R., Yang, G., Simon, G. P., Zhang, X., Zhang, L. and Wang, H. (2019c) Enhancement of desalination performance of thin-film nanocomposite membrane by cellulose nanofibers, *J. Membr. Sci.*, 592, 117363.
- Liu, S., Zeng, T. H., Hofmann, M., Burcombe, E., Wei, J., Jiang, R., Kong, J. and Chen, Y. (2011) Antibacterial Activity of Graphite, Graphite Oxide, Graphene Oxide, and Reduced Graphene Oxide: Membrane and Oxidative Stress, *ACS Nano*, 5(9), 6971–6980.
- Liu, X., Tang, Y., Gao, J., Luo, Q., Zeng, Z. and Wang, Q. (2019d) Room-temperature synthesis of novel polymeric nanocluster with emissions and its Cu²⁺ recognition performance, *J. Lumin.*, 205, 142–147.
- Liu, Y., Tan, J., Choi, W., Hsu, J.-H., Han, D. S., Han, A., Abdel-Wahab, A. and Yu, C. (2018) Influence of nanoparticle inclusions on the performance of reverse osmosis membranes, *Environ. Sci. Water Res. Technol.*, 4(3), 411–420.
- Loeb, S. and Sourirajan, S. (1963) Sea Water Demineralization by Means of Osmotic Membrane, *Adv. Chem. Ser.*, 38, 117–132.
- Lonsdale, H. K. and Podall, H. E. (1972) *Reverse Osmosis Membrane Research*. in Lonsdale, H. K. and Podall, H. E. (eds.) *Springer, Boston, MA*. Boston, MA: Springer US.
- Lou, Y., Liu, G., Liu, S., Shen, J. and Jin, W. (2014) A facile way to prepare ceramic-supported graphene oxide composite membrane via silane-graft modification, *Appl. Surf. Sci.*, 307, 631–637.

- Lu, X., Arias Chavez, L. H., Romero-Vargas Castrillón, S., Ma, J. and Elimelech, M. (2015) Influence of active layer and support layer surface structures on organic fouling propensity of thin-film composite forward osmosis membranes, *Environ. Sci. Technol.*, 49(3), 1436–1444.
- Lu, X., Feng, X., Werber, J. R., Chu, C., Zucker, I., Kim, J.-H., Osuji, C. O. and Elimelech, M. (2017) Enhanced antibacterial activity through the controlled alignment of graphene oxide nanosheets, *Proc. Natl. Acad. Sci.*, 114(46), E9793–E9801.
- Luo, T., Young, R. and Reig., P. (2015) Aqueduct Projected Water Stress Country Rankings, *World Resour. Inst.*, 1–16.
- Ma, J., Ping, D. and Dong, X. (2017) Recent Developments of Graphene Oxide-Based Membranes: A Review, *Membranes (Basel)*, 7(3), 52.
- Mai, Z., Gui, S., Fu, J., Jiang, C., Ortega, E., Zhao, Y., Tu, W., Mickols, W. and Van der Bruggen, B. (2019) Activity-derived model for water and salt transport in reverse osmosis membranes: A combination of film theory and electrolyte theory, *Desalination*, 469, 114094.
- Malaeb, L. and Ayoub, G. M. (2011) Reverse osmosis technology for water treatment: State of the art review, *Desalination*, 267(1), 1–8.
- Mangadlao, J. D., Santos, C. M., Felipe, M. J. L., De Leon, A. C. C., Rodrigues, D. F. and Advincula, R. C. (2015) On the antibacterial mechanism of graphene oxide (GO) Langmuir-Blodgett films, *Chem. Commun.*, 51(14), 2886–2889.
- Mariën, H. and Vankelecom, I. F. J. (2018) Optimization of the ionic liquid-based interfacial polymerization system for the preparation of high-performance, low-fouling RO membranes, *J. Membr. Sci.*, 556, 342–351.
- Matthews, T. D., Yan, H., Cahill, D. G., Coronell, O. and Mariñas, B. J. (2013) Growth dynamics of interfacially polymerized polyamide layers by diffuse reflectance spectroscopy and Rutherford backscattering spectrometry, *J. Membr. Sci.*, 429, 71–80.
- Mayyahi, A. Al (2018) Thin-film composite (TFC) membrane modified by hybrid ZnO-graphene nanoparticles (ZnO-Gr NPs) for water desalination, *J. Environ. Chem. Eng.*, 6(1), 1109–1117.
- Mekonnen, M. M. and Hoekstra, A. Y. (2016) Sustainability: Four billion people facing severe water scarcity, *Sci. Adv.*, 2(2), 1–7.

- Min, Y., Wang, T., Zhang, Y. and Chen, Y. (2011) The synthesis of poly(p-phenylenediamine) microstructures without oxidant and their effective adsorption of lead ions, *J. Mater. Chem.*, 21(18), 6683–6689.
- Murthy, Z. V. P. and Gupta, S. K. (1997) Estimation of mass transfer coefficient using a combined nonlinear membrane transport and film theory model, *Desalination*, 109(1), 39–49.
- Naaktgeboren, A. J., Snijders, G. J. and Gons, J. (1988) Characterization of a new reverse osmosis composite membrane for industrial application, *Desalination*, 68(2–3), 223–242.
- Nagaraj, V., Skillman, L., Li, D. and Ho, G. (2018) Review – Bacteria and their extracellular polymeric substances causing biofouling on seawater reverse osmosis desalination membranes, *J. Environ. Manage.*, 223, 586–599.
- Nakajima, T. and Matsuo, Y. (1994) Formation process and structure of graphite oxide, *Carbon N. Y.*, 32(3), 469–475.
- Nakao, S. and Kimura, S. (1982) Models of membrane transport phenomena and their applications for ultrafiltration data., *J. Chem. Eng. JAPAN*, 15(3), 200–205.
- Nan, Q., Li, P. and Cao, B. (2016) Fabrication of positively charged nanofiltration membrane via the layer-by-layer assembly of graphene oxide and polyethylenimine for desalination, *Appl. Surf. Sci.*, 387, 521–528.
- Ng, K. C., Thu, K., Oh, S. J., Ang, L., Shahzad, M. W. and Ismail, A. Bin (2015) Recent developments in thermally-driven seawater desalination: Energy efficiency improvement by hybridization of the MED and AD cycles, *Desalination*, 356, 255–270.
- Ng, Z. C., Lau, W. J. and Ismail, A. F. (2020) GO/PVA-integrated TFN RO membrane: Exploring the effect of orientation switching between PA and GO/PVA and evaluating the GO loading impact, *Desalination*, 496, 114538.
- Ng, Z. C., Lau, W. J., Matsuura, T. and Ismail, A. F. (2021) Thin film nanocomposite RO membranes: Review on fabrication techniques and impacts of nanofiller characteristics on membrane properties, *Chem. Eng. Res. Des.*, 165, 81–105.
- Ng, Z., Chong, C., Lau, W., Karaman, M. and Ismail, A. F. (2019) Boron removal and antifouling properties of thin-film nanocomposite membrane incorporating PECVD-modified titanate nanotubes, *J. Chem. Technol. Biotechnol.*, 94(9), 2772–2782.

- Oizerovich-Honig, R., Raim, V. and Srebnik, S. (2010) Simulation of thin film membranes formed by interfacial polymerization, *Langmuir*, 26(1), 299–306.
- Ong, C. S., Goh, P. S., Lau, W. J., Misdan, N. and Ismail, A. F. (2016) Nanomaterials for biofouling and scaling mitigation of thin film composite membrane: A review, *Desalination*, 393, 2–15.
- Oren, Y. S. and Biesheuvel, P. M. (2018) Theory of Ion and Water Transport in Reverse-Osmosis Membranes, *Phys. Rev. Appl.*, 9(2), 024034.
- Otitoju, T. A., Saari, R. A. and Ahmad, A. L. (2018) Progress in the modification of reverse osmosis (RO) membranes for enhanced performance, *J. Ind. Eng. Chem.*, 67, 52–71.
- Pang, R. and Zhang, K. (2018) Fabrication of hydrophobic fluorinated silica-polyamide thin film nanocomposite reverse osmosis membranes with dramatically improved salt rejection, *J. Colloid Interface Sci.*, 510, 127–132.
- Park, S.-H., Kim, S. H., Park, S.-J., Ryoo, S., Woo, K., Lee, J. S., Kim, T.-S., Park, H.-D., Park, H., Park, Y.-I., Cho, J. and Lee, J.-H. (2016) Direct incorporation of silver nanoparticles onto thin-film composite membranes via arc plasma deposition for enhanced antibacterial and permeation performance, *J. Membr. Sci.*, 513, 226–235.
- Park, S.-J., Kwon, S. J., Kwon, H.-E., Shin, M. G., Park, S.-H., Park, H., Park, Y.-I., Nam, S.-E. and Lee, J.-H. (2018) Aromatic solvent-assisted interfacial polymerization to prepare high performance thin film composite reverse osmosis membranes based on hydrophilic supports, *Polymer (Guildf.)*, 144, 159–167.
- Perera, D. H. N., Song, Q., Qiblawey, H. and Sivaniah, E. (2015) Regulating the aqueous phase monomer balance for flux improvement in polyamide thin film composite membranes, *J. Membr. Sci.*, 487, 74–82.
- Perreault, F., de Faria, A. F., Nejati, S. and Elimelech, M. (2015) Antimicrobial Properties of Graphene Oxide Nanosheets: Why Size Matters, *ACS Nano*, 9(7), 7226–7236.
- Perreault, F., Tousley, M. E. and Elimelech, M. (2014) Thin-Film Composite Polyamide Membranes Functionalized with Biocidal Graphene Oxide Nanosheets, *Environ. Sci. Technol. Lett.*, 1(1), 71–76.
- Qasim, M., Badrelzaman, M., Darwish, N. N., Darwish, N. A. and Hilal, N. (2019) Reverse osmosis desalination: A state-of-the-art review, *Desalination*, 459, 59–104.

- Qin, D., Liu, Z., Bai, H. and Sun, D. D. (2017) Three-dimensional architecture constructed from a graphene oxide nanosheet–polymer composite for high-flux forward osmosis membranes, *J. Mater. Chem. A*, 5(24), 12183–12192.
- Qiu, S., Wu, L., Zhang, L., Chen, H. and Gao, C. (2009) Preparation of reverse osmosis composite membrane with high flux by interfacial polymerization of MPD and TMC, *J. Appl. Polym. Sci.*, 112(4), 2066–2072.
- Raaijmakers, M. J. T. and Benes, N. E. (2016) Current trends in interfacial polymerization chemistry, *Prog. Polym. Sci.*, 63, 86–142.
- Rahimpour, A., Madaeni, S. S., Amirinejad, M., Mansourpanah, Y. and Zereshti, S. (2009) The effect of heat treatment of PES and PVDF ultrafiltration membranes on morphology and performance for milk filtration, *J. Membr. Sci.*, 330(1–2), 189–204.
- Rajakumaran, R., Boddu, V., Kumar, M., Shalaby, M. S., Abdallah, H. and Chetty, R. (2019) Effect of ZnO morphology on GO-ZnO modified polyamide reverse osmosis membranes for desalination, *Desalination*, 467, 245–256.
- Regula, C., Carretier, E., Wyart, Y., Sergent, M., Gésan-Guizieu, G., Ferry, D., Vincent, A., Boudot, D. and Moulin, P. (2013) Ageing of ultrafiltration membranes in contact with sodium hypochlorite and commercial oxidant: Experimental designs as a new ageing protocol, *Sep. Purif. Technol.*, 103, 119–138.
- Reid, C. E. and Breton, E. J. (1959) Water and ion flow across cellulosic membranes, *J. Appl. Polym. Sci.*, 1(2), 133–143.
- Rezaeian, M. S., Mousavi, S. M., Saljoughi, E. and Akhlaghi Amiri, H. A. (2020) Evaluation of thin film composite membrane in production of ionically modified water applied for enhanced oil recovery, *Desalination*, 474, 114194.
- Riley, R. L., Fox, R. L., Lyons, C. R., Milstead, C. E., Seroy, M. W. and Tagami, M. (1976) Spiral-wound poly (ether/amide) thin-film composite membrane systems, *Desalination*, 19(1–3), 113–126.
- Rodríguez, B. E., Armendariz-Ontiveros, M. M., Quezada, R., Huitrón-Segovia, E. A., Estay, H., García García, A. and García, A. (2020) Influence of Multidimensional Graphene Oxide (GO) Sheets on Anti-Biofouling and Desalination Performance of Thin-Film Composite Membranes: Effects of GO Lateral Sizes and Oxidation Degree, *Polymers (Basel)*, 12(12), 2860.

- Roh, I. J., Greenberg, A. R. and Khare, V. P. (2006) Synthesis and characterization of interfacially polymerized polyamide thin films, *Desalination*, 191(1–3), 279–290.
- Roh, I. J. and Khare, V. P. (2002) Investigation of the specific role of chemical structure on the material and permeation properties of ultrathin aromatic polyamides, *J. Mater. Chem.*, 12(8), 2334–2338.
- Roshan, A. and Kumar, M. (2020) Water end-use estimation can support the urban water crisis management: A critical review, *J. Environ. Manage.*, 268(336), 110663.
- Safarpour, M., Khataee, A. and Vatanpour, V. (2015) Thin film nanocomposite reverse osmosis membrane modified by reduced graphene oxide/TiO₂ with improved desalination performance, *J. Membr. Sci.*, 489, 43–54.
- Saleem, H. and Zaidi, S. J. (2020) Nanoparticles in reverse osmosis membranes for desalination: A state of the art review, *Desalination*, 475(July 2019), 114171.
- Sanchez, V. C., Jachak, A., Hurt, R. H. and Kane, A. B. (2012) Biological interactions of graphene-family nanomaterials: An interdisciplinary review, *Chem. Res. Toxicol.*, 25(1), 15–34.
- Seah, M. Q., Lau, W. J., Goh, P. S., Tseng, H.-H., Wahab, R. A. and Ismail, A. F. (2020) Progress of Interfacial Polymerization Techniques for Polyamide Thin Film (Nano)Composite Membrane Fabrication: A Comprehensive Review, *Polymers (Basel)*, 12(12), 2817.
- Seo, K., Kim, M. and Kim, D. H. (2015) *Re-derivation of Young's Equation, Wenzel Equation, and Cassie-Baxter Equation Based on Energy Minimization. Surface Energy*. InTech.
- Service, R. F. (2006) Desalination Freshens Up, *Science*, 313(5790), 1088–1090.
- Seyyed Shahabi, S., Azizi, N. and Vatanpour, V. (2019) Synthesis and characterization of novel g-C₃N₄ modified thin film nanocomposite reverse osmosis membranes to enhance desalination performance and fouling resistance, *Sep. Purif. Technol.*, 215, 430–440.
- Seyyed Shahabi, S., Azizi, N., Vatanpour, V. and Yousefimehr, N. (2020) Novel functionalized graphitic carbon nitride incorporated thin film nanocomposite membranes for high-performance reverse osmosis desalination, *Sep. Purif. Technol.*, 235, 116134.

- Shah, A. A., Cho, Y. H., Choi, H., Nam, S.-E., Kim, J. F., Kim, Y., Park, Y.-I. and Park, H. (2019) Facile integration of halloysite nanotubes with bioadhesive as highly permeable interlayer in forward osmosis membranes, *J. Ind. Eng. Chem.*, 73, 276–285.
- Shamaila, S., Sajjad, A. K. L. and Iqbal, A. (2016) Modifications in development of graphene oxide synthetic routes, *Chem. Eng. J.*, 294, 458–477.
- Shao, F., Dong, L., Dong, H., Zhang, Q., Zhao, M., Yu, L., Pang, B. and Chen, Y. (2017) Graphene oxide modified polyamide reverse osmosis membranes with enhanced chlorine resistance, *J. Membr. Sci.*, 525, 9–17.
- Shao, G., Lu, Y., Wu, F., Yang, C., Zeng, F. and Wu, Q. (2012) Graphene oxide: the mechanisms of oxidation and exfoliation, *J. Mater. Sci.*, 47(10), 4400–4409.
- Sharma, R. R. and Chellam, S. (2005) Temperature effects on the morphology of porous thin film composite nanofiltration membranes, *Environ. Sci. Technol.*, 39(13), 5022–5030.
- Shen, L., Hung, W., Zuo, J., Zhang, X., Lai, J.-Y. and Wang, Y. (2019) High-performance thin-film composite polyamide membranes developed with green ultrasound-assisted interfacial polymerization, *J. Membr. Sci.*, 570–571, 112–119.
- Shen, L., Zhang, X., Zuo, J. and Wang, Y. (2017) Performance enhancement of TFC FO membranes with polyethyleneimine modification and post-treatment, *J. Membr. Sci.*, 534, 46–58.
- Sheng, Y., Tang, X., Peng, E. and Xue, J. (2013) Graphene oxide based fluorescent nanocomposites for cellular imaging, *J. Mater. Chem. B*, 1(4), 512–521.
- Shenvi, S. S., Isloor, A. M. and Ismail, A. F. (2015) A review on RO membrane technology: Developments and challenges, *Desalination*, 368, 10–26.
- Shi, G. M. and Chung, T. S. (2013) Thin film composite membranes on ceramic for pervaporation dehydration of isopropanol, *J. Membr. Sci.*, 448, 34–43.
- Shi, J., Wu, W., Xia, Y., Li, Z. and Li, W. (2018) Confined interfacial polymerization of polyamide-graphene oxide composite membranes for water desalination, *Desalination*, 441, 77–86.
- Shi, M., Wang, Z., Zhao, S., Wang, J. and Wang, S. (2017) A support surface pore structure re-construction method to enhance the flux of TFC RO membrane, *J. Membr. Sci.*, 541, 39–52.

- Sinclair, T. R., Robles, D., Raza, B., van den Hengel, S., Rutjes, S. A., de Roda Husman, A. M., de Grooth, J., de Vos, W. M. and Roesink, H. D. W. (2018) Virus reduction through microfiltration membranes modified with a cationic polymer for drinking water applications, *Colloids Surfaces A Physicochem. Eng. Asp.*, 551, 33–41.
- Singh, P. S., Joshi, S. V., Trivedi, J. J., Devmurari, C. V., Rao, A. P. and Ghosh, P. K. (2006) Probing the structural variations of thin film composite RO membranes obtained by coating polyamide over polysulfone membranes of different pore dimensions, *J. Membr. Sci.*, 278(1–2), 19–25.
- Smith, E., Hendren, K., Haag, J., Foster, E. and Martin, S. (2019) Functionalized Cellulose Nanocrystal Nanocomposite Membranes with Controlled Interfacial Transport for Improved Reverse Osmosis Performance, *Nanomaterials*, 9(1), 125.
- Song, X., Zhou, Q., Zhang, T., Xu, H. and Wang, Z. (2016) Pressure-assisted preparation of graphene oxide quantum dot-incorporated reverse osmosis membranes: antifouling and chlorine resistance potentials, *J. Mater. Chem. A*, 4(43), 16896–16905.
- Song, Y., Sun, P., Henry, L. L. and Sun, B. (2005) Mechanisms of structure and performance controlled thin film composite membrane formation via interfacial polymerization process, *J. Membr. Sci.*, 251(1–2), 67–79.
- Spiegler, K. S. S. and Kedem, O. (1966) Thermodynamics of hyperfiltration (reverse osmosis): criteria for efficient membranes, *Desalination*, 1(4), 311–326.
- Staudenmaier, L. (1898) Method for the preparation of graphitic acid, *Berichte der Dtsch. Chem. Gesellschaft*, 31(2), 1481–1487.
- Tang, C. Y., Kwon, Y.-N. and Leckie, J. O. (2007) Probing the nano- and micro-scales of reverse osmosis membranes—A comprehensive characterization of physiochemical properties of uncoated and coated membranes by XPS, TEM, ATR-FTIR, and streaming potential measurements, *J. Membr. Sci.*, 287(1), 146–156.
- Tang, S. and Zheng, J. (2018) Antibacterial Activity of Silver Nanoparticles: Structural Effects, *Adv. Healthc. Mater.*, 7(13), 1–10.

- Uhlenbrook, S., Milettor, M., Connor, R., Koncagul, E., Abete, V., Tonsini, M. and Lobach, S. (2020) *The United Nations World Water Development Report 2020: Water and Climate Change*. Paris, France: United Nations Educational, Scientific and Cultural Organization.
- Vatanpour, V., Safarpour, M., Khataee, A., Zarrabi, H., Yekavalangi, M. E. and Kaviani, M. (2017) A thin film nanocomposite reverse osmosis membrane containing amine-functionalized carbon nanotubes, *Sep. Purif. Technol.*, 184, 135–143.
- Vatanpour, V., Sheydaei, M. and Esmaceli, M. (2017) Box-Behnken design as a systematic approach to inspect correlation between synthesis conditions and desalination performance of TFC RO membranes, *Desalination*, 420, 1–11.
- Verbeke, R., Gómez, V. and Vankelecom, I. F. J. (2017) Chlorine-resistance of reverse osmosis (RO) polyamide membranes, *Prog. Polym. Sci.*, 72, 1–15.
- Wada, Y. and Bierkens, M. F. P. (2014) Sustainability of global water use: past reconstruction and future projections, *Environ. Res. Lett.*, 9(10), 104003.
- Wan Azelee, I., Goh, P. S., Lau, W. J., Ismail, A. F., Rezaei-DashtArzhandi, M., Wong, K. C. and Subramaniam, M. N. (2017) Enhanced desalination of polyamide thin film nanocomposite incorporated with acid treated multiwalled carbon nanotube-titania nanotube hybrid, *Desalination*, 409, 163–170.
- Wang, F., Zheng, T., Xiong, R., Wang, P. and Ma, J. (2019a) Strong improvement of reverse osmosis polyamide membrane performance by addition of ZIF-8 nanoparticles: Effect of particle size and dispersion in selective layer, *Chemosphere*, 233, 524–531.
- Wang, H., Li, L., Zhang, X. and Zhang, S. (2010) Polyamide thin-film composite membranes prepared from a novel triamine 3,5-diamino-N-(4-aminophenyl)-benzamide monomer and m-phenylenediamine, *J. Membr. Sci.*, 353(1–2), 78–84.
- Wang, H., Zhang, Q. and Zhang, S. (2011) Positively charged nanofiltration membrane formed by interfacial polymerization of 3,3',5,5'-biphenyl tetraacyl chloride and piperazine on a poly(acrylonitrile) (PAN) support, *J. Membr. Sci.*, 378(1–2), 243–249.
- Wang, J., Dlamini, D. S., Mishra, A. K., Pendergast, M. T. M., Wong, M. C. Y., Mamba, B. B., Freger, V., Verliefe, A. R. D. and Hoek, E. M. V. (2014) A critical review of transport through osmotic membranes, *J. Membr. Sci.*, 454, 516–537.

- Wang, J., Xu, R., Yang, F., Kang, J., Cao, Y. and Xiang, M. (2018) Probing influences of support layer on the morphology of polyamide selective layer of thin film composite membrane, *J. Membr. Sci.*, 556, 374–383.
- Wang, L., Wang, N., Li, J., Li, J., Bian, W. and Ji, S. (2016a) Layer-by-layer self-assembly of polycation/GO nanofiltration membrane with enhanced stability and fouling resistance, *Sep. Purif. Technol.*, 160, 123–131.
- Wang, R., Low, Z.-X., Liu, S., Wang, Y., Murthy, S., Shen, W. and Wang, H. (2020) Thin-film composite polyamide membrane modified by embedding functionalized boron nitride nanosheets for reverse osmosis, *J. Membr. Sci.*, 611, 118389.
- Wang, T., Lu, J., Mao, L. and Wang, Z. (2016b) Electric field assisted layer-by-layer assembly of graphene oxide containing nanofiltration membrane, *J. Membr. Sci.*, 515, 125–133.
- Wang, W., Li, Y., Wang, W., Gao, B. and Wang, Z. (2019b) Palygorskite/silver nanoparticles incorporated polyamide thin film nanocomposite membranes with enhanced water permeating, antifouling and antimicrobial performance, *Chemosphere*, 236, 124396.
- Wang, Y., Gao, B., Li, S., Jin, B., Yue, Q. and Wang, Z. (2019c) Cerium oxide doped nanocomposite membranes for reverse osmosis desalination, *Chemosphere*, 218, 974–983.
- Wei, J., Liu, X., Qiu, C., Wang, R. and Tang, C. Y. (2011) Influence of monomer concentrations on the performance of polyamide-based thin film composite forward osmosis membranes, *J. Membr. Sci.*, 381(1–2), 110–117.
- Wen, Y., Chen, Y., Wu, Z., Liu, M. and Wang, Z. (2019) Thin-film nanocomposite membranes incorporated with water stable metal-organic framework CuBTri for mitigating biofouling, *J. Membr. Sci.*, 582, 289–297.
- Wen, Y., Zhang, X., Li, X., Wang, Z. and Tang, C. Y. (2020) Metal–Organic Framework Nanosheets for Thin-Film Composite Membranes with Enhanced Permeability and Selectivity, *ACS Appl. Nano Mater.*, 3(9), 9238–9248.
- Wenzel, R. N. (1936) Resistance of solid surfaces to wetting by water, *Ind. Eng. Chem.*, 28(8), 988–994.
- Widjaya, A., Hoang, T., Stevens, G. W. and Kentish, S. E. (2012) A comparison of commercial reverse osmosis membrane characteristics and performance under alginate fouling conditions, *Sep. Purif. Technol.*, 89, 270–281.

- Wijmans, J. G. and Baker, R. W. (1995) The solution-diffusion model: a review, *J. Membr. Sci.*, 107(1–2), 1–21.
- Williams, P. M., Ahmad, M., Connolly, B. S. and Oatley-Radcliffe, D. L. (2015) Technology for freeze concentration in the desalination industry, *Desalination*, 356, 314–327.
- Wissler, M. (2006) Graphite and carbon powders for electrochemical applications, *J. Power Sources*, 156(2), 142–150.
- Xia, S., Yao, L., Zhao, Y., Li, N. and Zheng, Y. (2015) Preparation of graphene oxide modified polyamide thin film composite membranes with improved hydrophilicity for natural organic matter removal, *Chem. Eng. J.*, 280, 720–727.
- Xie, M. and Gray, S. R. (2016) Transport and accumulation of organic matter in forward osmosis-reverse osmosis hybrid system: Mechanism and implications, *Sep. Purif. Technol.*, 167, 6–16.
- Xie, W., Geise, G. M., Freeman, B. D., Lee, H. S., Byun, G. and McGrath, J. E. (2012) Polyamide interfacial composite membranes prepared from m-phenylene diamine, trimesoyl chloride and a new disulfonated diamine, *J. Membr. Sci.*, 403–404, 152–161.
- Xu, C., Shao, F., Yi, Z., Dong, H., Zhang, Q., Yu, J., Feng, J., Wu, X., Zhang, Q., Yu, L. and Dong, L. (2019) Highly chlorine resistance polyamide reverse osmosis membranes with oxidized graphitic carbon nitride by ontology doping method, *Sep. Purif. Technol.*, 223, 178–185.
- Xu, G.-R., Wang, J.-N. and Li, C.-J. (2013) Strategies for improving the performance of the polyamide thin film composite (PA-TFC) reverse osmosis (RO) membranes: Surface modifications and nanoparticles incorporations, *Desalination*, 328, 83–100.
- Xu, J., Wang, Z., Wang, J. and Wang, S. (2015) Positively charged aromatic polyamide reverse osmosis membrane with high anti-fouling property prepared by polyethylenimine grafting, *Desalination*, 365, 398–406.
- Yan, H., Miao, X., Xu, J., Pan, G., Zhang, Y., Shi, Y., Guo, M. and Liu, Y. (2015) The porous structure of the fully-aromatic polyamide film in reverse osmosis membranes, *J. Membr. Sci.*, 475, 504–510.
- Yan, W., Shi, M., Wang, Z., Zhao, S. and Wang, J. (2019a) Confined growth of skin layer for high performance reverse osmosis membrane, *J. Membr. Sci.*, 585, 208–217.

- Yan, X., Huo, L., Ma, C. and Lu, J. (2019b) Layer-by-layer assembly of graphene oxide-TiO₂ membranes for enhanced photocatalytic and self-cleaning performance, *Process Saf. Environ. Prot.*, 130, 257–264.
- Yang, X., Du, Y., Zhang, X., He, A. and Xu, Z.-K. (2017) Nanofiltration Membrane with a Mussel-Inspired Interlayer for Improved Permeation Performance, *Langmuir*, 33(9), 2318–2324.
- Yang, Z., Guo, H. and Tang, C. Y. (2019) The upper bound of thin-film composite (TFC) polyamide membranes for desalination, *J. Membr. Sci.*, 590, 117297.
- Yao, Z., Guo, H., Yang, Z., Lin, C., Zhu, B., Dong, Y. and Tang, C. Y. (2018) Reactable substrate participating interfacial polymerization for thin film composite membranes with enhanced salt rejection performance, *Desalination*, 436, 1–7.
- Yin, J. and Deng, B. (2015) Polymer-matrix nanocomposite membranes for water treatment, *J. Membr. Sci.*, 479, 256–275.
- Yin, J., Kim, E. S., Yang, J. and Deng, B. (2012) Fabrication of a novel thin-film nanocomposite (TFN) membrane containing MCM-41 silica nanoparticles (NPs) for water purification, *J. Membr. Sci.*, 423–424, 238–246.
- Yin, J., Zhu, G. and Deng, B. (2016) Graphene oxide (GO) enhanced polyamide (PA) thin-film nanocomposite (TFN) membrane for water purification, *Desalination*, 379, 93–101.
- You, M., Li, W., Pan, Y., Fei, P., Wang, H., Zhang, W., Zhi, L. and Meng, J. (2019) Preparation and characterization of antibacterial polyamine-based cyclophosphazene nanofiltration membranes, *J. Membr. Sci.*, 592(August), 117371.
- Youssef, P. G., Al-Dadah, R. K. and Mahmoud, S. M. (2014) Comparative analysis of desalination technologies, *Energy Procedia*, 61, 2604–2607.
- Yu, W., Sisi, L., Haiyan, Y. and Jie, L. (2020) Progress in the functional modification of graphene/graphene oxide: a review, *RSC Adv.*, 10(26), 15328–15345.
- Zaidi, S. M. J., Fadhillah, F., Khan, Z. and Ismail, A. F. (2015) Salt and water transport in reverse osmosis thin film composite seawater desalination membranes, *Desalination*, 368, 202–213.
- Zargar, M., Hartanto, Y., Jin, B. and Dai, S. (2017) Polyethylenimine modified silica nanoparticles enhance interfacial interactions and desalination performance of thin film nanocomposite membranes, *J. Membr. Sci.*, 541, 19–28.

- Zarshenas, K., Jiang, G., Zhang, J., Jauhar, M. A. and Chen, Z. (2020) Atomic scale manipulation of sublayer with functional TiO₂ nanofilm toward high-performance reverse osmosis membrane, *Desalination*, 480, 114342.
- Zeng, G., Lian, G., Zhang, Y., Gan, L., Zhou, Y., Qiu, J., van der Bruggen, B. and Shen, J. (2016) Potential applications of abandoned aromatic polyamide reverse osmosis membrane by hypochlorite degradation, *RSC Adv.*, 6(15), 12263–12271.
- Zhai, X., Ye, J., He, Y., Ahmatjan, Z., Zhang, Y., Lin, S., Wang, C., Hu, X. and Meng, J. (2020) Antibacterial Thin Film Composite Polyamide Membranes Prepared by Sequential Interfacial Polymerization, *Macromol. Mater. Eng.*, 305(7), 2000114.
- Zhai, Z., Zhao, N., Dong, W., Li, P., Sun, H. and Niu, Q. J. (2019) In Situ Assembly of a Zeolite Imidazolate Framework Hybrid Thin-Film Nanocomposite Membrane with Enhanced Desalination Performance Induced by Noria–Polyethyleneimine Codeposition, *ACS Appl. Mater. Interfaces*, 11(13), 12871–12879.
- Zhang, A., Zhang, Y., Pan, G., Xu, J., Yan, H. and Liu, Y. (2017a) In situ formation of copper nanoparticles in carboxylated chitosan layer: Preparation and characterization of surface modified TFC membrane with protein fouling resistance and long-lasting antibacterial properties, *Sep. Purif. Technol.*, 176, 164–172.
- Zhang, L., Shi, G.-Z., Qiu, S., Cheng, L.-H. and Chen, H.-L. (2011) Preparation of high-flux thin film nanocomposite reverse osmosis membranes by incorporating functionalized multi-walled carbon nanotubes, *Desalin. Water Treat.*, 34(1–3), 19–24.
- Zhang, Q., Zhang, Z., Dai, L., Wang, H., Li, S. and Zhang, S. (2017b) Novel insights into the interplay between support and active layer in the thin film composite polyamide membranes, *J. Membr. Sci.*, 537, 372–383.
- Zhang, T., Li, Z., Wang, W., Wang, Y., Gao, B. and Wang, Z. (2019) Enhanced antifouling and antimicrobial thin film nanocomposite membranes with incorporation of Palygorskite/titanium dioxide hybrid material, *J. Colloid Interface Sci.*, 537, 1–10.
- Zhang, Y., Ruan, H., Guo, C., Liao, J., Shen, J. and Gao, C. (2020a) Thin-film nanocomposite reverse osmosis membranes with enhanced antibacterial resistance by incorporating p-aminophenol-modified graphene oxide, *Sep. Purif. Technol.*, 234, 116017.

- Zhang, Z., Huang, L., Wang, Y., Yang, K., Du, Y., Wang, Y., Kipper, M. J., Belfiore, L. A. and Tang, J. (2020b) Theory and simulation developments of confined mass transport through graphene-based separation membranes, *Phys. Chem. Chem. Phys.*, 22(11), 6032–6057.
- Zhao, D. L., Japip, S., Zhang, Y., Weber, M., Maletzko, C. and Chung, T. S. (2020a) Emerging thin-film nanocomposite (TFN) membranes for reverse osmosis: A review, *Water Res.*, 173, 115557.
- Zhao, D. L., Yeung, W. S., Zhao, Q. and Chung, T. (2020b) Thin-film nanocomposite membranes incorporated with UiO-66-NH₂ nanoparticles for brackish water and seawater desalination, *J. Membr. Sci.*, 604, 118039.
- Zhao, H., Qiu, S., Wu, L., Zhang, L., Chen, H. and Gao, C. (2014) Improving the performance of polyamide reverse osmosis membrane by incorporation of modified multi-walled carbon nanotubes, *J. Membr. Sci.*, 450, 249–256.
- Zhao, S., Yao, Y., Ba, C., Zheng, W., Economy, J. and Wang, P. (2015) Enhancing the performance of polyethylenimine modified nanofiltration membrane by coating a layer of sulfonated poly(ether ether ketone) for removing sulfamerazine, *J. Membr. Sci.*, 492, 620–629.
- Zhao, W., Liu, H., Liu, Y., Jian, M., Gao, L., Wang, H. and Zhang, X. (2018) Thin-film nanocomposite forward-osmosis membranes on hydrophilic microfiltration support with an intermediate layer of graphene oxide and multiwall carbon nanotube, *ACS Appl. Mater. Interfaces*, 10(40), 34464–34474.
- Zheng, Y., Liu, J., Liang, J., Jaroniec, M. and Qiao, S. Z. (2012) Graphitic carbon nitride materials: controllable synthesis and applications in fuel cells and photocatalysis, *Energy Environ. Sci.*, 5(5), 6717.
- Zhu, X., Cheng, X., Luo, X., Liu, Y., Xu, D., Tang, X., Gan, Z., Yang, L., Li, G. and Liang, H. (2020) Ultrathin Thin-Film Composite Polyamide Membranes Constructed on Hydrophilic Poly(vinyl alcohol) Decorated Support Toward Enhanced Nanofiltration Performance, *Environ. Sci. Technol.*, 54(10), 6365–6374.

LIST OF PUBLICATIONS

Journal with Impact Factor

1. **Ng, Z.C.**, Lau, W.J., Wong, K.C., Al-Ghouti, M.A. & Ismail, A.F. (2021). Improving Properties of Thin Film Nanocomposite Membrane through Polyethyleneimine Intermediate Layer: A Parametric Study. *Separation and Purification Technology*, 274, 119035. <https://doi.org/10.1016/j.seppur.2021.119035>. **(Q1, IF: 5.774)**
2. **Ng, Z.C.**, Lau, W.J., Matsuura, T. & Ismail, A.F (2021). Thin Film Nanocomposite RO Membranes: Review on Fabrication Techniques and Impacts of Nanofiller Characteristics on Membrane Properties. *Chemical Engineering Research and Design*, 165, 81-105. <https://doi.org/10.1016/j.cherd.2020.10.003>. **(Q2, IF: 3.35)**
3. **Ng, Z.C.**, Lau, W.J. & Ismail, A.F (2020). GO/PVA-integrated TFN RO membrane: Exploring the effect of orientation switching between PA and GO/PVA and evaluating the GO loading impact. *Desalination*, 496, 114538. <https://doi.org/10.1016/j.desal.2020.114538>. **(Q1, IF: 7.098)**
4. **Ng, Z.C.**, Lau, W.J., Kartohardjono, S. & Ismail, A.F (2020). Comprehensive studies of membrane rinsing on the physicochemical properties and separation performance of TFC RO membranes. *Desalination*, 491, 114345. <https://doi.org/10.1016/j.desal.2020.114345>. **(Q1, IF: 7.098)**
5. **Ng, Z.C.**, Chong, C.Y., Sunarya, M.H., Lau, W.J., Liang, Y.Y., Fong, S.Y. & Ismail, A.F (2020). Reuse potential of spent RO membrane for NF and UF process. *Membrane and Water Treatment*, 11, 1-11. <http://dx.doi.org/10.12989/mwt.2020.11.5.323>. **(Q4, IF: 0.854)**

6. **Ng, Z.C.**, Chong, C.Y., Lau, W.J., Karaman, M. & Ismail, A.F (2019). Boron removal and antifouling properties of thin-film nanocomposite membrane incorporating PECVD-modified titanate nanotubes. *Journal of Chemical Technology and Biotechnology*, 94, 2772-2782. <https://doi.org/10.1002/jctb.6044>. **(Q2, IF: 2.75)**

7. Abdullah, N., Yusof, N., Abu Shah, M.H., Wan Ikhsan, S.N., **Ng, Z.C.**, Maji, S., Lau, W.J., Jaafar, J., Ismail, A.F. & Ariga, K (2019). Hydrous ferric oxide nanoparticles hosted porous polyethersulfone adsorptive membrane: chromium (VI) adsorptive studies and its applicability for water/wastewater treatment. *Environmental Science and Pollution Research*, 26, 20386–20399. <https://doi.org/10.1007/s11356-019-05208-9>. **(Q2, IF: 3.056)**

8. Lee, W.J., **Ng, Z.C.**, Hubadillah, S.K., Goh, P.S., Lau, W.J., Othman, M.H.D., Ismail, A.F. & Hilal, N (2020). Fouling mitigation in forward osmosis and membrane distillation for desalination. *Desalination*, 480, 114348. <https://doi.org/10.1016/j.desal.2020.114338>. **(Q1, IF: 7.098)**